doi:10.1093/brain/aws075 Brain 2012: 135; 1964–1980 | 1964

BRAIN
A JOURNAL OF NEUROLOGY

Essential role of interleukin-6 in post-stroke angiogenesis

Karen Gertz,[1,2,*] Golo Kronenberg,[1,2,3,4,*] Roland E. Kälin,[5] Tina Baldinger,[1,2] Christian Werner,[6] Mustafa Balkaya,[1,2] Gina D. Eom,[5] Julian Hellmann-Regen,[3] Jan Kröber,[1,2] Kelly R. Miller,[5] Ute Lindauer,[1,7] Ulrich Laufs,[6] Ulrich Dirnagl,[1,2,8] Frank L. Heppner[5,8] and Matthias Endres[1,2,8]

1 Department of Neurology, Charité – Universitätsmedizin Berlin, 10117 Berlin, Germany
2 Centre for Stroke Research Berlin, Charité – Universitätsmedizin Berlin, 10117 Berlin, Germany
3 Department of Psychiatry, Charité – Universitätsmedizin Berlin, 14050 Berlin, Germany
4 Experimental and Clinical Research Centre, Max-Delbrück Centre and Charité – Universitätsmedizin Berlin, 13125 Berlin, Germany
5 Institute of Neuropathology, Charité – Universitätsmedizin Berlin, 10117 Berlin, Germany
6 Internal Medicine III, University Hospital of the Saarland, 66421 Homburg, Germany
7 Department of Neurosurgery, Klinikum rechts der Isar, Technical University Munich, 81675 Munich, Germany
8 Cluster of Excellence NeuroCure, Charité – Universitätsmedizin Berlin, 10117 Berlin, Germany

*These authors contributed equally to this work.

Correspondence to: Prof. Dr Matthias Endres,
Klinik und Poliklinik für Neurologie,
Charité – Universitätsmedizin Berlin,
Charitéplatz 1, 10117 Berlin,
Germany
E-mail: matthias.endres@charite.de

Ambivalent effects of interleukin-6 on the pathogenesis of ischaemic stroke have been reported. However, to date, the long-term actions of interleukin-6 after stroke have not been investigated. Here, we subjected interleukin-6 knockout (IL-$6^{-/-}$) and wild-type control mice to mild brain ischaemia by 30-min filamentous middle cerebral artery occlusion/reperfusion. While ischaemic tissue damage was comparable at early time points, IL-$6^{-/-}$ mice showed significantly increased chronic lesion volumes as well as worse long-term functional outcome. In particular, IL-$6^{-/-}$ mice displayed an impaired angiogenic response to brain ischaemia with reduced numbers of newly generated endothelial cells and decreased density of perfused microvessels along with lower absolute regional cerebral blood flow and reduced vessel responsivity in ischaemic striatum at 4 weeks. Similarly, the early genomic activation of angiogenesis-related gene networks was strongly reduced and the ischaemia-induced signal transducer and activator of transcription 3 activation observed in wild-type mice was almost absent in IL-$6^{-/-}$ mice. In addition, systemic neoangiogenesis was impaired in IL-$6^{-/-}$ mice. Transplantation of interleukin-6 competent bone marrow into IL-$6^{-/-}$ mice (IL-6^{chi}) did not rescue interleukin-6 messenger RNA expression or the early transcriptional activation of angiogenesis after stroke. Accordingly, chronic stroke outcome in IL-6^{chi} mice recapitulated the major effects of interleukin-6 deficiency on post-stroke regeneration with significantly enhanced lesion volumes and reduced vessel densities. Additional *in vitro* experiments yielded complementary evidence, which showed that after stroke resident brain cells serve as the major source of interleukin-6 in a self-amplifying network. Treatment of primary cortical neurons, mixed glial cultures or immortalized brain endothelia with interleukin 6-induced robust interleukin-6 messenger RNA transcription in each case, whereas oxygen–glucose deprivation did not. However, oxygen–glucose deprivation of organotypic brain slices resulted in strong upregulation of interleukin-6 messenger RNA along with increased transcription of key angiogenesis-associated genes. In conclusion, interleukin-6 produced locally by resident brain cells promotes post-stroke angiogenesis and thereby affords long-term histological and functional protection.

Received April 30, 2011. Revised November 30, 2011. Accepted January 27, 2012. Advance Access publication April 3, 2012

Keywords: cerebral ischaemia; interleukin-6; inflammation; angiogenesis; regeneration

Abbreviations: BrdU = 5-bromo-2-deoxyuridine; GFP = green florescent protein; gp130 = glycoprotein 130; IL-6 = interleukin 6; MCAO = middle cerebral artery occlusion; STAT = signal transducer and activator of transcription; VEGF = vascular endothelial growth factor

Introduction

Interleukin-6 (IL-6) is an essential inflammatory mediator and significant elevations of IL-6 levels have been reported in stroke patients shortly after the ischaemic event (Acalovschi *et al.*, 2003; Smith *et al.*, 2004; Waje-Andreassen *et al.*, 2005). As a pleiotropic cytokine, IL-6 has pyrogenic properties and serves as an important messenger molecule between leucocytes, the vascular endothelium and resident cells of the parenchyma. Depending on the cellular context, IL-6 may exert an array of diverse and competing effects including anti-apoptotic, pro-proliferative, growth-inhibitory and differentiation-inducing effects. The biological activities of IL-6 are mediated by its dimeric membrane receptor. The IL-6 binding subunit, IL-6 receptor, exists in a membrane-bound and in a soluble form. Either of them bind IL-6 and then interact with the second subunit of the receptor complex, glycoprotein 130 (gp130) (Jüttler *et al.*, 2002). Dimerization of gp130 upon IL-6 binding leads to the activation of multiple intracellular signal transduction pathways including Janus kinase/signal transducer and activator of transcription (JAK/STAT) (Heinrich *et al.*, 2003; Nian *et al.*, 2004).

The source of the early surge in circulating IL-6 levels in stroke has been a matter of controversy for some time (Dziedzic *et al*., 2003). In fact, many cell types including all the major cell types in brain tissue are capable of synthesizing IL-6 (Woodroofe *et al.*, 1991; Schobitz *et al.*, 1993; Reyes *et al.*, 1999; Van Wagoner *et al.*, 1999). In stroke patients, peak plasma IL-6 levels correlate with larger infarct volume, increased stroke severity and less favourable outcome (Smith *et al.*, 2004). Ambivalent effects of IL-6 on the pathogenesis of ischaemic stroke have been reported. Untoward effects may especially relate to the pro-inflammatory and pyrogenic actions of IL-6, while there is also ample evidence for direct neuroprotective and neurotrophic actions (Suzuki *et al.*, 2009). For example, intracerebroventricular administration of recombinant IL-6 has been shown to reduce early ischaemic brain damage (Loddick *et al.*, 1998). Similarly, disruption of IL-6 signalling by intraperitoneal injection of an anti-mouse IL-6 receptor monoclonal antibody has been reported to exacerbate ischaemic damage at 24 h after a 45-min period of middle cerebral artery occlusion (MCAO) (Yamashita *et al.*, 2005). In contrast, two studies comparing acute stroke outcome between IL-$6^{+/+}$ and IL-$6^{-/-}$ mice yielded comparable lesion sizes unless body temperature was controlled by external warming (Clark *et al*., 2000; Herrmann *et al*., 2003).

Both beneficial and detrimental effects of neuroinflammation in response to ischaemic injury have been described (Planas *et al.*, 2006). The 'Janus face' of inflammation after brain ischaemia is best exemplified by the fact that the same factors may contribute to tissue damage or protection depending on the temporospatial context of their expression. So far, experimental stroke studies have mainly investigated short-term survival paradigms, although chronic end points may be of much greater clinical relevance. In contrast to the acute phase, in which stroke severity directly correlates with early neuron loss, in the chronic phase complex regenerative responses such as angiogenesis critically impinge on outcome (Gertz *et al*., 2006; Chen *et al.*, 2009; Navaratna *et al.*, 2009). The so-called 'clean-up hypothesis' posits that inflammation and angiogenesis are intricately linked in the post-ischaemic brain for the removal and replacement of damaged tissue (Manoonkitiwongsa *et al.*, 2001; Zhao *et al.*, 2006). Although IL-6 has been implicated in wound healing and angiogenesis in peripheral tissue (Gallucci *et al.*, 2000; Lin *et al.*, 2003), more long-term effects of IL-6 after stroke have not been investigated.

In the current study, we provide complementary evidence that resident brain cells serve as the major source of increased IL-6 levels early after stroke. We demonstrate that IL-6 promotes STAT3 phosphorylation and early activation of angiogenesis-related gene transcription, which leads to increased angiogenesis and improved cerebral blood flow during the delayed phases after stroke. IL-6 thereby confers improved long-term outcome with reduced lesion sizes and better functional recovery after mild stroke.

Materials and methods

Cell culture experiments

Primary neuronal cultures of rat cerebral cortex were obtained from foetal Wistar rats at embryonic Day 17 as described previously (Lautenschlager *et al.*, 2000). Briefly, cerebral cortex was dissected, incubated for 15 min in trypsin/EDTA (0.05/0.02% w/v in phosphate-buffered saline) at 37°C, rinsed twice with phosphate-buffered saline and once with dissociation medium (modified Eagle's medium with 10% foetal calf serum, 10 mM HEPES, 44 mM glucose, 100 U/ml penicillin/streptomycin, 2 mM L-glutamine, 0.025 IU/ml insulin), dissociated by Pasteur pipette in dissociation medium, pelleted by centrifugation (at 225 *g* for 2 min), redissociated in starter medium [Neurobasal medium and supplement B27 (Gibco), 100 U/ml penicillin/streptomycin, 0.5 mM L-glutamine, 25 µM glutamate], and plated in 6-well plates at a density of 1.5×10^6 cells/well. Wells were pretreated by incubation with poly-L-lysine (2.5 µg/ml in phosphate-buffered saline; Biochrom) at 4°C overnight and then carefully rinsed with phosphate-buffered saline twice. Cultures were fed on *in vitro* Day 4 with cultivating medium (starter medium without glutamate) by replacing 30% of the medium. Experiments were performed after *in vitro* Days 8–12.

Primary mixed glial cultures were isolated from cortex of post-natal Day 1–3 mice. Briefly, cerebral cortex was dissected, incubated for 15 min in trypsin/EDTA (0.05/0.02% w/v in phosphate-buffered saline) at 37°C, rinsed twice with phosphate-buffered saline and once with a standard cultivation medium consisting of Dulbecco's modified Eagle medium with stable glutamine (Biochrom FG 0435) containing 10% foetal calf serum, 100 U/ml penicillin/streptomycin and 1 mM sodium pyruvate (Biochrom). Tissue was dissociated by pipetting. After centrifugation at 225 *g* for 5 min, the pellet was

redissociated in cultivation medium and filtered through a nylon mesh (pore size of 70 μm; BD Biosciences). The resulting cell suspension was plated in 6-well plates (two brains per plate). Wells were pretreated by incubation with poly-L-lysine (2.5 μg/ml in phosphate-buffered saline; Biochrom) at room temperature for 2 h and then carefully rinsed twice with phosphate-buffered saline. After 24 h, medium was changed. Experiments were performed after *in vitro* Days 8–12.

Immortalized murine brain endothelial bEnd.3 cells (ATCC) were cultured in Dulbecco's modified Eagle medium (ATCC) containing 10% foetal calf serum. Cells were seeded at 2.5×10^5 cells/well in a 6-well plate for 48 h, after which experiments were begun. The MTT assay, based on the cleavage of the yellow tetrazolium salt MTT (Sigma) to purple formazan by mitochondrial enzymes in metabolically active cells, was performed as described (Lautenschlager *et al*., 2000).

Organotypic brain slice cultures were prepared from post-natal Day 5–7 mice as previously described (Heppner *et al*., 2005). After decapitation, the brain was removed and the hippocampi were dissected and transversely sectioned at 350 μm using a McIlwain tissue chopper (The Mickle Laboratory Engineering Co. Ltd.). Slices were immediately transferred to a porous membrane (Millipore Millicell inserts, PICIM 03050) and maintained in culture. Cell culture medium contained 50% minimal essential medium (PAA), 25% horse serum (Invitrogen) and 25% Hank's balanced salt solution (Invitrogen) supplemented with glucose, B27 supplement, penicillin and streptomycin. Medium was exchanged after 24 h in culture and then every 3 days. Experiments were performed on *in vitro* Day 9.

Oxygen–glucose deprivation was essentially performed as described previously (Endres *et al.*, 2004). Briefly, after removal of the medium, cultures were subjected to oxygen–glucose deprivation in a balanced salt solution within an anaerobic chamber (0.3% O_2; INVIVO$_2$ 400, Ruskinn Life Sciences). In the control condition, cells were transferred to a balanced salt solution with 20 mM D-glucose in normoxic atmosphere with 5% CO_2 for the same duration of time as in the oxygen–glucose deprivation condition. Primary cortical neurons were subjected to moderate oxygen–glucose deprivation (3 h; e.g. Nagai *et al.*, 2001) whereas mixed glial cultures and bEnd.3 cells were subjected to prolonged oxygen–glucose deprivation (5 h; e.g. Andjelkovic *et al.*, 2003). In order to be able to detect the additional effect of oxygen–glucose deprivation in cultured brain slices, which already show microglial activation under normal culture conditions (tissue injury at upper and lower surfaces), we performed oxygen–glucose deprivation over 6 h. Lactate dehydrogenase activity was measured as described (Harms *et al.*, 2000). For IL-6 stimulation experiments in primary cortical neurons, which are differentiated in serum-free medium, we used recombinant human IL-6 (Sigma) along with human soluble IL-6 receptor a (sIL-6Ra; 100 ng/ml; Peprotech) and 10% foetal calf serum. Mixed glial cultures, bEnd.3 cells and brain slices were stimulated with recombinant mouse IL-6 (R&D Systems). Cells were harvested 24 h after stimulation for quantitative polymerase chain reaction analyses.

Animals and drug treatment

All experimental procedures conformed to institutional guidelines and were approved by an official committee. The generation of IL-6 knockout mice (IL-$6^{-/-}$) has been described in detail previously (Kopf *et al.*, 1994). Briefly, IL-6 deficient mice had been backcrossed on a C57BL/6J background for >10 generations (Chourbaji *et al.*, 2006). Male IL-$6^{-/-}$ mice and littermate controls (8–10 weeks old and weighing 18–22 g; Charles River) were group housed with *ad libitum* access to food and water. Nucleoside analogue 5-bromo-2-deoxyuridine (BrdU) was administered intraperitoneally at a dose of 50 μg/g body weight at a concentration of 10 mg/ml (Kronenberg *et al.*, 2003).

Model of cerebral ischaemia

Mice were anaesthetized for induction with 1.5% isoflurane and maintained in 1.0% isoflurane in 69% N_2O and 30% O_2 using a vaporizer. Left MCAO was essentially performed as described elsewhere (Endres *et al.*, 2000*a*). In brief, brain ischaemia was induced with an 8.0 nylon monofilament coated with a silicone resin/hardener mixture (Xantopren M Mucosa and Activator NF Optosil Xantopren, Haereus Kulzer). The filament was introduced into the internal carotid artery up to the anterior cerebral artery. Thereby, the middle cerebral artery and anterior choroidal arteries were occluded. The filament was removed after 30 min to allow reperfusion. Core temperature was maintained at 36.5 ± 0.5°C with a feed-back temperature control unit during, but not after, MCAO.

India ink perfusion

The technique used for visualization of brain angioarchitecture was essentially as described previously (Maeda *et al.*, 1998; Endres *et al.*, 2004). Briefly, deeply anaesthetized mice were transcardially perfused with 10% (v/v) India ink (Pelikan) in 6% (w/v) gelatin in warm (38°C) distilled water. After decapitation, brains were post-fixed in 4% paraformaldehyde overnight in the skull, after which they were carefully collected. Development of the posterior communicating artery of both hemispheres was scored as follows: 0, absent; 1, present but poorly developed (hypoplastic); and 2, well formed. Additionally, the number of anastomoses per hemisphere between the territory of the anterior and middle cerebral arteries was counted.

Disc neovascularization model

Disc neovascularization was measured 2 weeks after implantation of polyvinyl alcohol sponges (Rippey) covered with nitrocellulose cell-impermeable filters (Millipore). Perfusion was performed with fluorescent microspheres (0.2 μm; Invitrogen) as described (Laufs *et al*., 2004; Gertz *et al*., 2006).

Quantification of endothelial progenitor cells

The spleen serves as a haematopoietic organ in adult mice. Spleens were harvested 48 h after 30 min MCAO/reperfusion. Mononuclear cells were isolated by Ficoll density gradient centrifugation as described (Werner *et al.*, 2007). Four million mononuclear cells per animal were plated on fibronectin-coated 24-well plates in duplicate assays. Cells were cultivated in endothelial-selective basal medium (Lonza) to select for endothelial progenitor cells. After 4 days in culture, adherent cells were incubated with 1,1′-dioctadecyl-3,3,3′,3′-tetramethylindocarbocyanine-labelled acetylated low density lipoprotein (DiLDL, 2.4 μg/ml; CellSystems) for 1 h and stained using fluorescein isothiocyanate-labelled *Ulex europaeus* agglutinin I (lectin, 10 μg/ml; Sigma-Aldrich) for 4 h. Nuclei were counterstained with 4′,6-diamidino-2-phenylindole (DAPI; Linaris). Three random high-power fields were captured from each coverslip using a Nikon DS-Ri1 digital camera mounted on a Nikon Eclipse E600 fluorescence microscope. The number of DiLDL-lectin-positive nucleated cells was counted using NIS 3.0 BR software by an investigator blind to the genotype of the donor animal.

Generation of bone marrow chimeric mice

Bone marrow chimeras were generated as described previously (Grathwohl *et al.*, 2009). Briefly, donor cells were obtained from tibia and femur of TgN(beta-act-EGFP)1Osb mice (Jackson Laboratories). After lethal irradiation with 950 rad, wild-type and IL-$6^{-/-}$ mice were injected intravenously with 7×10^6 bone marrow cells and subsequently treated with an antibiotic (enrofloxacin; 0.01% Baytril®, Bayer Vital). Successful reconstitution was defined as >90% engraftment of blood leukocytes by fluorescence-activated cell sorting analysis.

Histochemistry and immunohistochemistry

After an overdose of anaesthetic, animals were transcardially perfused with physiological saline followed by 4% paraformaldehyde in 0.1 M phosphate buffer, pH 7.4. Brains were dissected from the skulls and post-fixed overnight. Before sectioning from a dry ice-cooled copper block on a sliding microtome (Leica), the brains were transferred to 30% sucrose in 0.1 M phosphate buffer pH 7.4 until they sank. Brains were cut in the coronal plane in 40-μm thick sections. Sections were stored at −20°C in cryoprotectant solution (25% ethylene glycol, 25% glycerol and 0.05 M phosphate buffer). Sections were stained using free-floating immunohistochemistry and prepared for BrdU detection by incubation with 2 N HCl for 30 min at 37°C as described in detail previously (Kronenberg *et al.*, 2003). Primary antibodies were applied in the following concentrations: anti-BrdU (rat, 1:500, Harlan Seralab), anti-NeuN (mouse, 1:100, Chemicon), anti-vWF (rabbit, 1:200, Chemicon), anti-Iba1 (rabbit, 1:500, Wako), anti-green fluorescent protein (GFP) (rabbit, 1:200, Abcam; goat, 1:100, Acris), anti-glial fibrillary acidic protein (guinea pig, 1:1000, Advanced ImmunoChemical) and anti-cd31 (rabbit, 1:50, Abcam). Immunohistochemistry followed the peroxidase method with biotinylated secondary antibodies (all 1:500; Jackson ImmunoResearch Laboratories), ABC Elite reagent (Vector Laboratories) and 3,3′-diaminobenzidine (Sigma) as chromogen. For immunofluorescence FITC-, RhodX- or Cy5-conjugated secondary antibodies were all used at a concentration of 1:250. Fluorescent sections were coverslipped in polyvinyl alcohol with diazabicyclooctane (DABCO) as anti-fading agent.

Quantification and imaging

The number of BrdU+ cells per volume was assessed using StereoInvestigator® software (MicroBrightfield) as described previously (Gertz *et al.*, 2006). Briefly, in defined reference sections (i.e. interaural +4.9, +4.1 and +3.3 mm) the ischaemic lesion and the corresponding area in the contralateral hemisphere were delineated at ×100 magnification and cells counted at ×200 magnification. Phenotypic analysis of BrdU-labelled cells was performed using a spectral confocal microscope (TCS SP2; Leica). Appropriate gain and black level settings were determined on control slices stained with secondary antibodies alone.

Density of perfused vessels

Evans blue (Sigma-Aldrich; 2% in saline) was administered intravenously and allowed to circulate for 5 min. In some animals, acetazolamide (30 mg/kg body weight; Sigma-Aldrich) was coadministered intravenously 5 min before sacrifice. Animals were decapitated and brains cut into 10 μm coronal cryostat sections and digitized with a cooled CCD-camera (Dage-MTI) which was attached to a fluorescence microscope. Images of whole brain sections at microscopic resolution were obtained by joining together single camera images using tiled-field mapping software (MCID Elite, InterFocus). Regions of interest were specified with the technique of density slicing, including the setting of target acceptance criteria (Göbel *et al.*, 1990).

Measurement of cerebral blood flow

Regional absolute cerebral blood flow was quantified using the ^{14}C-iodoantipyrine technique as explained previously (Endres *et al.*, 2003).

Dissection of brain tissue

For the analyses described below, a complete 4 mm coronal section was dissected from the left (i.e. ischaemic) hemisphere (approximately +5.8 mm to +1.8 mm from interaural line) and stored at −80°C until further use.

Western blotting

Cellular fractionation was performed as described previously (Harms *et al.*, 2007). Briefly, tissue was homogenized in 20 μl/mg ice-cold cell lysis buffer [10 mM HEPES, pH 7.5, 2 mM $MgCl_2$, 1 mM EDTA, 1 mM EGTA, 10 mM KCl, 1 mM DTT, 50 mM NaF, 2 mM Na_3VO_4, 1 × Protease Inhibitor Cocktail (Roche)]. Five microlitres of 10% NP-40 was added per 100 μl of cell lysis buffer. The suspension was vortexed and centrifuged for 30 s at 13 000 *g* and 4°C. The supernatant was taken as the cytosolic fraction. The pellet was washed in cell lysis buffer and then resuspended in 5 μl/mg nuclear extraction buffer [25 mM HEPES pH 7.5, 500 mM NaCl, 1 mM DTT, 50 mM NaF, 2 mM Na_3VO_4, 10% glycerol, 0.2% NP-40, 5 mM $MgCl_2$, 1 × Protease Inhibitor Cocktail (Roche)]. The suspension was vortexed, sonicated and centrifuged for 5 min at 13 000 *g* and 4°C. The supernatant was taken as the nuclear fraction. Protein concentration was determined by Bicinchoninic acid Protein Assay (Pierce). Equal amounts of protein were loaded on 10% Tris–HEPES gels (Pierce) and blotted onto polyvinylidene fluoride membranes. Blots were probed with primary and secondary antibodies and developed by chemiluminescent detection methods. Where necessary, blots were stripped and reprobed by a second primary antibody. Antibodies were used in the following concentrations: rabbit anti-pSTAT3 (Tyr705) (Cell Signaling, 1:400), mouse anti-pERK1/ERK2 (Thr202/Tyr204) (Cell Signaling, 1:400), rabbit anti-pAKT (Thr308) (Cell Signaling, 1:400), rabbit anti-Hdac1 (Santa Cruz, 1:1000), mouse anti-GAPDH (Chemicon, 1:40 000), mouse anti-STAT3 (Cell Signaling, 1:500), rabbit anti-ERK1/ERK2 (Sigma, 1:60 000) rabbit anti-AKT (Cell Signaling, 1:1000), anti-rabbit horseradish peroxidase (Pierce, 1:5000) and anti-mouse horseradish peroxidase (Amersham, 1:5000).

Enzyme-linked immunosorbent assay

Vascular endothelial growth factor (VEGF) levels in serum and IL-6 concentrations in rethawed homogenates of brain tissue were analysed using commercial ELISA kits in principle according to the manufacturers' instructions (R&D Systems and Biosource, respectively).

Messenger RNA isolation and polymerase chain reactions

Tissue was homogenized and total RNA extracted using TRIzol® reagent (Invitrogen). For polymerase chain reaction amplification, we used gene-specific primers (Table 1) and Light Cycler® FastStart DNA

Table 1 Primer sequences used in quantitative real-time polymerase chain reaction

Gene	Sense	Antisense
Tpp2	CTTCTATCCAAAGGCTCTCAAGG	CTCTCCAGGTCTCACCATCATG
Nos3	CAGGACTGCACAGGAAATGTTC	AGCACATCAAAGCGGCCATTTC
Kdr	GCATGGTCTTCTGTGAGGCAAAG	GAGAGTGCCAGGTGAAATCAAGC
IL-6	GAGGATACCACTCCCAACAGACC	AAGTGCATCATCGTTGTTCATACA
IL6-IMR	TTCCATCCAGTTGCCTTCTTGG	TTCTCATTTCCACGATTTCCCAG
IL-6 R	GCTGGCAGCACCCTGAGACC	TCCAAGGAGTGCCCGTGACC
gp130	TGAAGCTGTCTTAGCGTGGG	GGTGACCACTGGGCAATATG
Anxa2	GTACGACTCCATGAAGGGCAAG	GTACAGCAGTGCCTTCTGGTAG
Thbs1	GACTAGGTGTCCTGTTCCTGTTG	CTGGATAGATCTTGGCCCTTCAC
Cx3cl1	GAATCCCAGTGGCTTTGCTCATC	CATTGTCCACCCGCTTCTCAAAC
Bai3	CTCAAGTCTGCAATCTGACCAG	GTCCCGTAAGGTGATACACAAG
Cxcl4	CGATGGAGATCTTAGCTGTGTG	CATTCTTCAGGGTGGCTATGAG
Dicer1	CTCACTCGGATCTCAAGGTTGG	CACTCCTGAGAATTCGCTCCAG
C1galt1	CATGCTTCACAATGACCCTCATG	GATAGAGGTTCTCAGCAACGTC
Adamts1	GATCCAGAGCACTATGACACTGC	CATCGAGGCCATCAGATGAGAATC
Edn1	CTTCTGCCACCTGGACATCATC	GCTATTGCTGATGGCCTCCAAC
Gfap	GACAACTTTGCACAGGACCTCG	CCACTCCTCTGTCTCTTGCATG
rat IL-6	GAGACTTCACAGAGGATACCAC	CAGTGCATCATCGCTGTTCATAC
Jam-1	CTCTTCACGTCTATGATCCTGG	GTCACAGAACTGAACGTGATGC
ICAM1	CAGTCCGCTGTGCTTTGAGAAC	GCACCGTGAATGTGATCTCCTTG
PECAM-1	CACGATTGAGTACGAGGTGAAG	CCATGAGCACAAAGTTCTCGTTG
VE-Cadherin	GCAATGGCAGGCCCTAACTTTC	CAGCAAACTCTCCTTGGAGCAC

Master SYBR Green I (Roche Diagnostics). Polymerase chain reaction conditions were as follows: preincubation 95°C, 10 min; 95°C, 15 s, primer-specific annealing temperature, 10 s, 72°C, 15 s (45 cycles). Crossing points of amplified products were determined using the Second Derivative Maximum Method (Light Cycler Version 3.5, Roche). Quantification of messenger RNA expression was relative to tripeptidyl peptidase (Tpp) 2 (Nishida *et al.*, 2006). Specificity of polymerase chain reaction products was checked using melting curve analysis and electrophoresis in a 1.5% agarose gel.

Microarray analysis

Tissue dissected from the ischaemic hemisphere (see above) was used for gene expression analysis using the GeneChip® Mouse Gene 1.0 ST Array essentially as described previously (Pohlers *et al.*, 2005). A detailed description of target preparation and hybridization is available online at: http://www.charite.de/lfgc. Data analysis was performed using Microarray Suite Version 5.0 software and Data Mining Tool Version 2.0 software (Affymetrix). Detailed information on the microarray experiments reported here, including protocols, the data sets and the platform used, were submitted to the European Bioinformatics Institute (www.ebi.ac.uk/miamexpress) under the experiment name 'Essential role of interleukin-6 for post-stroke angiogenesis' (ArrayExpress accession: E-MEXP-2547).

Functional outcome

Rotarod

To assess general fitness and motor coordination, a Rotarod test was used (TSE Sytems). Mice were placed on an accelerating rotating rod (acceleration from 2 rpm to 40 rpm within 5 min) and a stop-clock was started. When the mice dropped and touched the sensing platform below, the stop-clock stopped automatically. Each animal performed three trials.

Pole test

The animal was placed head upward near the top of a vertical steel pole which was covered with tape so as to create a rough surface. The time until the mouse had completely turned around on the pole so as to face downward was recorded ('t turn'). The time required to reach the floor with all four paws ('t floor') was also measured. If the animal reached the floor without completely having turned around, the time to reach the floor was also attributed to t turn (Ji *et al.*, 2009).

Corner test

The corner test was devised as a sensitive method to detect ischaemia-induced postural and sensorimotor symmetries. The test was performed as described (Zhang *et al.*, 2002).

Statistical analysis

Experiments were carried out in a blinded fashion. Data are presented as mean ± SEM. Unless otherwise indicated, groups were compared by ANOVA with level of significance set at 0.05 and two-tailed *P*-values.

Results

Early upregulation of angiogenesis-associated genes is reduced in IL-6$^{-/-}$ mice after transient mild brain ischaemia

First, we investigated changes in IL-6 expression in the ischaemic brain of wild-type mice following 30 min MCAO/reperfusion. IL-6 messenger RNA (Fig. 1A) and protein levels (Fig. 1B) showed a

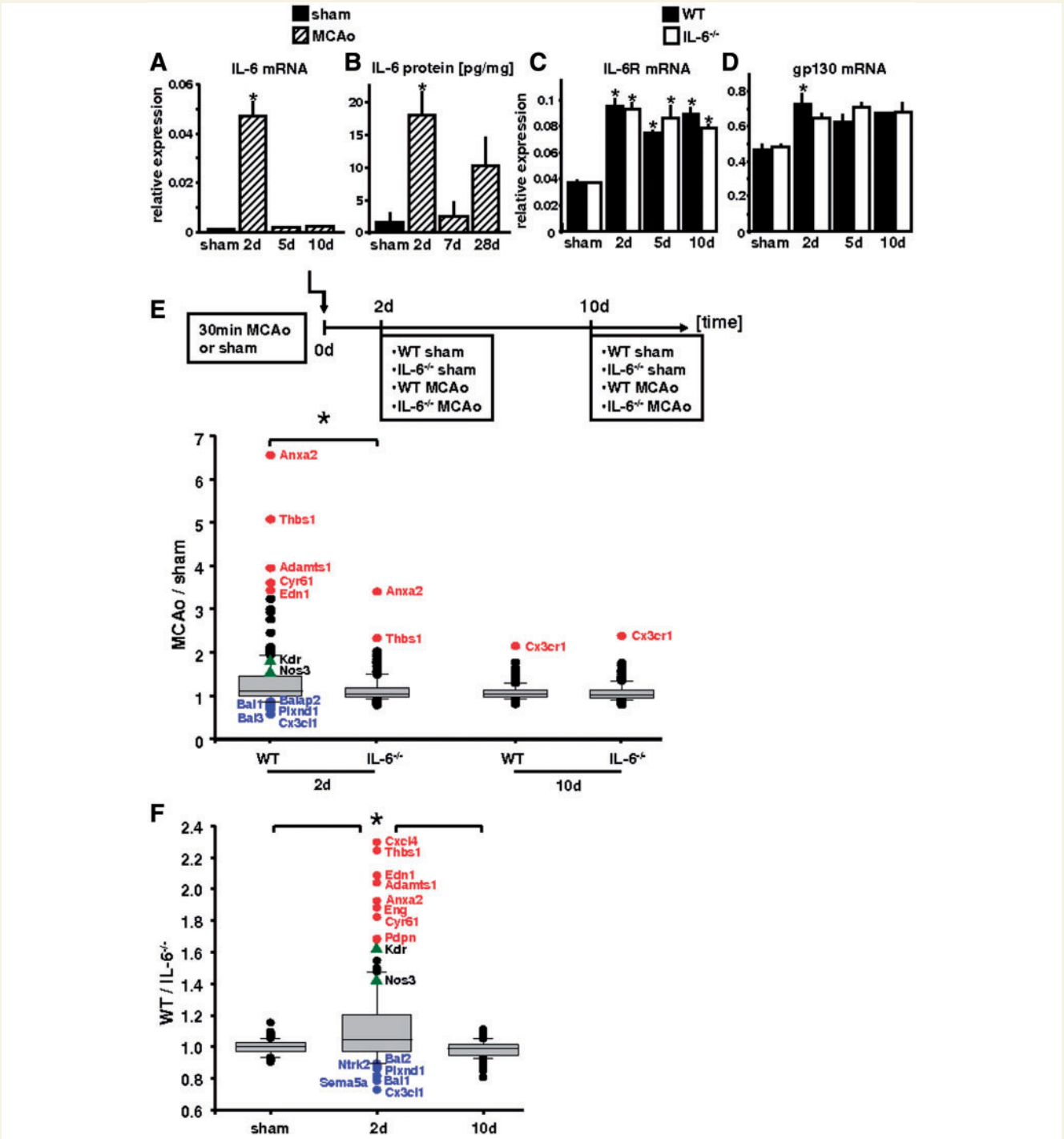

Figure 1 Early upregulation of angiogenesis-related genes after mild brain ischaemia is attenuated in IL-$6^{-/-}$ mice. IL-6 messenger RNA (**A**) and protein expression levels (**B**) were measured in ischaemic brain of wild-type mice after 30 min MCAO/reperfusion. (**C** and **D**) Transcription of IL-6 receptor (**C**) and gp130 (**D**) messenger RNA was assessed in IL-$6^{-/-}$ mice and wild-type littermate controls. Note that IL-6 receptor and, to a lesser extent gp130, showed prolonged upregulation after transient brain ischaemia. Relative messenger RNA expression is reported as the value normalized to tripeptidyl peptidase 2 (Tpp2) for each sample. $n = 3$–6 animals per group. *$P < 0.05$ versus sham. (**E** and **F**) IL-$6^{-/-}$ mice and wild-type littermate controls were exposed to 30 min MCAO/reperfusion or sham operation. Animals were euthanized at 2 and 10 days after brain ischaemia. Unpooled samples of ipsilateral brain tissue were processed for microarray analysis. Messenger RNA expression of 162 angiogenesis-associated genes (for detailed summary of gene expression see Supplementary Table 1) was analysed. (**E**) Ratio of gene expression of angiogenesis-associated genes in MCAO versus sham-operated animals. Note that at 2 days after 30 min MCAO/reperfusion, angiogenesis-associated genes as a class show significantly stronger activation in wild-type relative to IL-$6^{-/-}$ mice. (**F**) Significant increase in the ratio of gene expression in wild-type to IL-$6^{-/-}$ mice at 2 days after MCAO/reperfusion. Note that the expression of angiogenesis-related genes is comparable in IL-$6^{-/-}$ mice and wild-type controls both in the

(continued)

significant early upregulation at 48 h after stroke. Using IL-6$^{-/-}$ mice and wild-type controls, we then studied transcription of IL-6 receptor and gp130 messenger RNA at different time points after 30-min MCAO (Fig. 1C and D). Interestingly, transcription of IL-6 receptor and, to a lesser extent, also transcription of gp130 messenger RNA showed an early, yet sustained upregulation after ischaemia.

In a 2 × 2 design, we subjected IL-6$^{-/-}$ mice and wild-type controls to 30 min MCAO/reperfusion or sham operation. An early (i.e. 48 h after the experimental intervention) as well as a subacute time point (i.e. 10 days) were investigated (Fig. 1E and F). RNA was isolated from the (ischaemic) left hemisphere and transcript abundance levels quantified by hybridization to complementary DNA microarrays. Analysis of messenger RNA expression of 162 angiogenesis-associated genes revealed an early angiogenic response in wild-type mice at 2 days after MCAO/reperfusion. ANOVA on ranks showed that this early induction of angiogenesis-related genes was significantly reduced in IL-6$^{-/-}$ mice. By contrast, angiogenic genes as a class did not differ between genotypes either under sham conditions or at 10 days after MCAO/reperfusion (Fig. 1E and F; for the complete list of genes see Supplementary Table 1; for a graphic illustration of the fold change in each of the 162 genes refer to Supplementary Fig. 1). Quantitative real-time polymerase chain reaction was used to confirm the data obtained from microarray analysis. We evaluated example genes showing either: (i) the strongest increase; or (ii) the strongest decrease; and additionally (iii) genes that did not show significant messenger RNA expression changes in microarray experiments. There was a high concordance between quantitative polymerase chain reaction and microarray results (Supplementary Fig. 2A–I). In addition, we quantified VEGF receptor 2 (Kdr) and endothelial NO synthase (Nos3) messenger RNA (Fig. 1E and F). Again, reverse-transcription polymerase chain reactions confirmed an early upregulation of Kdr and Nos3 messenger RNA in the ischaemic hemisphere of wild-type mice, which was significantly attenuated in IL-6$^{-/-}$ mice (Supplementary Fig. 2H and I).

In a different set of animals, we quantified expression of key angiogenesis-associated genes at 28 days after transient mild brain ischaemia (Supplementary Fig. 3). Compared with the 48 h time point, the magnitudes of the changes in gene expression at this chronic time point after MCAO were generally quite small (<2-fold messenger RNA induction for any of the genes investigated). Furthermore, a clear pattern of genotype effects was no longer discernible (Supplementary Fig. 3).

We studied the effects of IL-6 deficiency on gene regulation of adhesion molecules: junctional adhesional molecule-1 (Jam-1), intercellular adhesion molecule 1 (ICAM1), platelet endothelial cell adhesion molecule-1 (PECAM-1) and vascular endothelial (VE)-cadherin at 48 h after 30 min MCAO. A role for these candidate adhesion molecules in the regulation of angiogenesis has been clearly documented (DeLisser *et al.*, 1997; Carmeliet *et al.*, 1999; Naik *et al.*, 2003; Kevil *et al.*, 2004; Azari *et al.*, 2011). Interestingly, we observed a similar pattern of regulation as reported above for key angiogenesis-related genes with a blunted response in IL-6$^{-/-}$ mice (Supplementary Fig. 4).

Finally, at 2 days post-event, VEGF protein concentrations in serum were also ~50% higher in wild-type than in IL-6$^{-/-}$ mice (151 ± 53 versus 78 ± 6 pg/ml; $n = 8$ animals per group). These genotype differences after stroke were not due to variabilities in brain vasculature (plasticity of the posterior communicating artery, number of anastomoses between anterior cerebral and middle cerebral arteries) nor to differences in acute cerebral blood flow during the MCAO procedure (Supplementary Fig. 5A–C).

In the mild (30 min) ischaemia model, neurons undergo delayed cell death whereas glia and endothelia remain largely intact (Katchanov *et al.*, 2003; Kronenberg *et al.*, 2005). In contrast, more severe (60 min) MCAO results in severe tissue damage (pannecrosis) in the middle cerebral artery territory (Endres *et al.*, 2000*b*; Harhausen *et al.*, 2010). We therefore evaluated regulation of key genes identified in the microarray experiments (see above) in a different set of mice subjected to 60 min MCAO. Similar to mild ischaemia, severe ischaemia led to significantly increased transcription of *Anxa2*, *Cxcl4*, *Thbs1*, *Edn1*, *Adamts1*, *Kdr* and *Nos3* at 2 days post-event. However, the genotype differences observed in the mild ischaemia model were not apparent with severe ischaemia (Supplementary Fig. 6).

Transplantation of IL-6 competent bone marrow into IL-6$^{-/-}$ mice does not rescue the angiogenic response after transient mild brain ischaemia

The source of the increased circulating IL-6 levels in stroke has been a matter of controversy for some time (Dziedzic *et al.*, 2003). In order to dissect the relative contribution of invading

Figure 1 Continued
sham condition and at 10 days after transient brain ischaemia (ratio ~1). Genes showing the strongest upregulation or the strongest downregulation are given in red and blue, respectively. Additionally, candidate genes VEGF receptor 2 (Kdr) and endothelial NO synthase (Nos3) confirmed by quantitative polymerase chain reaction (Supplementary Fig. 2H and I) are given (green triangles). $n = 24$ animals in total ($n = 3$ animals per intervention per genotype per time point). (**E**) and (**F**) represent the median, 10th, 25th, 75th and 90th percentiles as vertical boxes with error bars. One-way ANOVA on ranks followed by Newman–Keuls *post hoc* test. *$P < 0.05$.
Adamts1 = a disintegrin-like and metallopeptidase; Anxa2 = Annexin A2; Bai1 = brain-specific angiogenesis inhibitor 1; Baiap2 = brain-specific angiogenesis inhibitor 1-associated protein; Bai3 = brain-specific angiogenesis inhibitor 3; Cx3cl1 = chemokine C-X3-C ligand 1; Cxcl4 chemokine = C-X-C ligand 4; Cx3cr1 = chemokine C-X3-C receptor 1; Cyr61 = cystein rich protein 61; Edn1 = Endothelin 1; Eng = Endoglin; Kdr = VEGF receptor 2; Nos3 = endothelial NO synthase; Ntrk2 = neurotrophic tyrosine kinase receptor typ2; Pdpn = Podoplanin; Plxnd1 = Plexin D1; Sema5a = Semaphorin 5a; Thbs1 = Thrombospondin 1.

bone marrow-derived cells to the early surge of IL-6 levels as well as to the activation of angiogenesis-related gene networks after stroke, we performed 30 min MCAO in wild-type chimeric ($WT^{GFP} \rightarrow IL\text{-}6^{+/+}$; termed WT^{chi}) and $IL\text{-}6^{-/-}$ chimeric mice ($WT^{GFP} \rightarrow IL\text{-}6^{-/-}$; termed $IL\text{-}6^{chi}$) reconstituted with IL-6 competent, green fluorescent bone marrow. At 48 h after 30 min MCAO, the number of GFP-labelled cells in the infarct did not differ between genotypes (Fig. 2A and B). However, we did not detect any IL-6 gene transcription in the brains of either sham-operated or ischaemic $IL\text{-}6^{chi}$ mice. By contrast, IL-6 gene expression was strongly upregulated in the ischaemic brains of WT^{chi} animals (Fig. 2C and D). Although there was no apparent effect of MCAO, IL-6 messenger RNA was clearly detectable in spleens and livers of both WT^{chi} and $IL\text{-}6^{chi}$ mice (Fig. 2E and F). Further analysis of IL-6 protein levels in serum at 48 h after stroke showed a significant early increase in WT^{chi} mice whereas IL-6 levels in $IL\text{-}6^{chi}$ mice remained unchanged (Fig. 2G). We also studied gene expression of key angiogenesis-related genes identified in microarray experiments (see above). Again, in IL-6 competent WT^{chi} mice MCAO resulted in a substantial increase in all of these genes. In contrast, this early angiogenic response was strongly reduced in $IL\text{-}6^{chi}$ mice (Fig. 2H–L). Kdr and Nos3 showed a similar pattern of regulation (Fig. 2M and N).

Next, we compared chronic stroke outcome of $IL\text{-}6^{chi}$ mice with that of WT^{chi} mice (Fig. 2O–U). Although lesion sizes were significantly increased in $IL\text{-}6^{chi}$ mice (increase by ~75%; $n = 8$–9 animals per group), the number of bone marrow-derived (i.e. GFP-positive) cells in the ischaemic striatum was significantly reduced in $IL\text{-}6^{chi}$ compared with WT^{chi} mice at 4 weeks after stroke (Fig. 2O). Most interestingly, we again did not detect any IL-6 messenger RNA transcription in the ischaemic brains of $IL\text{-}6^{chi}$ mice despite the fact that the majority of GFP-labelled cells in the ischaemic striatum displayed immunoreactivity for microglia marker Iba1 (Fig. 2P; WT^{chi} mice: 156 out of 200 randomly selected GFP-positive cells; $IL\text{-}6^{chi}$ mice: 172 out of 200 randomly selected GFP-positive cells; $n = 5$ animals per group, respectively). Despite the complete absence of IL-6 messenger RNA transcription in brain, we again found clear evidence of IL-6 messenger RNA in spleens and livers of $IL\text{-}6^{chi}$ mice (Fig. 2Q–S). IL-6 levels in serum at 4 weeks after stroke did not differ between genotypes (WT^{chi} versus $IL\text{-}6^{chi}$) or treatment groups (sham versus MCAO) (Fig. 2T). As a functional parameter of angiogenesis, we assessed the density of perfused microvessels at 28 days after MCAO/reperfusion using endovascular, auto-fluorescent Evans blue staining and tiled-field imaging. In WT^{chi} mice, vessel density was increased significantly within the ischaemic striatum and significantly exceeded that of $IL\text{-}6^{chi}$ mice (Fig. 2U). These findings in WT^{chi} and $IL\text{-}6^{chi}$ mice recapitulate the genotype differences in neovascularization between wild-type and $IL\text{-}6^{-/-}$ mice detailed below (Fig. 5). Finally, we studied transcription of key angiogenesis-associated genes at 4 weeks. Compared with the 48 h time point, differences between groups were again relatively small. Furthermore, no clear pattern of genotype effects was discernable (not shown).

Taken together, these *in vivo* experiments highlight the importance of resident cells for the local production of IL-6 in the ischaemic brain and for neovascularization.

The upregulation of IL-6 after oxygen–glucose deprivation takes the form of a network response and is amplified by IL-6

To clarify the cellular source of IL-6 in brain after hypoxaemia further, we subjected neuronal and glial cultures to oxygen–glucose deprivation. IL-6 messenger RNA expression was assessed after 24 h. Neither primary cortical neurons nor mixed glial cultures containing astrocytes and microglia showed increased IL-6 gene transcription after oxygen–glucose deprivation despite significant increases in lactate dehydrogenase activity in culture medium (by ~110 and ~25%, respectively). Similarly, immortalized brain endothelia did not upregulate IL-6 gene expression after prolonged oxygen–glucose deprivation (Fig. 3A–C). By contrast, incubation with recombinant IL-6 resulted in significantly enhanced IL-6 messenger RNA expression in both primary cortical neurons and mixed glial cultures as well as in immortalized brain endothelial cells (Fig. 3D–F). Importantly, stimulation of bEnd.3 endothelia with recombinant IL-6 enhanced proliferation of these cells and led to significantly increased transcription of key angiogenesis-associated genes *Cxcl4*, *Thbs1*, *Edn1* and *Adamts1* (Fig. 3G–K). In contrast, messenger RNA expression of *Cxcl4*, *Thbs1*, *Edn1* and *Adamts1* in bEnd.3 cells was not upregulated by oxygen–glucose deprivation (not shown).

Finally, in order to study the effects of hypoxaemia on a more complex cellular network involving the interaction between different types of resident cells, we subjected organotypic brain slices to oxygen–glucose deprivation (Fig. 3L–P). Slices subjected to oxygen–glucose deprivation (increase of lactate dehydrogenase activity by ~50%) demonstrated clear upregulation of IL-6 messenger RNA along with increased transcription of key angiogenesis-associated genes (Fig. 3L–P). Coadministration of recombinant IL-6 after oxygen–glucose deprivation further significantly increased transcription of all these genes (Fig. 3L–P) demonstrating a gain of function mechanism.

In conclusion, these *in vitro* experiments demonstrate that IL-6 is upregulated in brain tissue after oxygen–glucose deprivation. This upregulation of IL-6 expression in the brain takes the form of a self-amplifying network response.

Loss of STAT3 activation in IL-6 deficient brain after mild transient ischaemia

Next, we characterized the intracellular pathways of IL-6 signalling after brain ischaemia *in vivo*. STAT3 functions as a transcription factor and an intracellular signal transducer that is important in cytokine signalling (Hirano *et al.*, 2000; Heinrich *et al.*, 2002; Levy *et al.*, 2002). At 24 h after MCAO/reperfusion, we did not detect a significant effect of either genotype or ischaemia on total STAT3 (Fig. 4). Tyrosine (705) phosphorylation of STAT3 is necessary for STAT3 dimerization, nuclear translocation and activation of gene transcription (Bromberg *et al.*, 2000). Phosphorylation of STAT3 at Tyr705 was

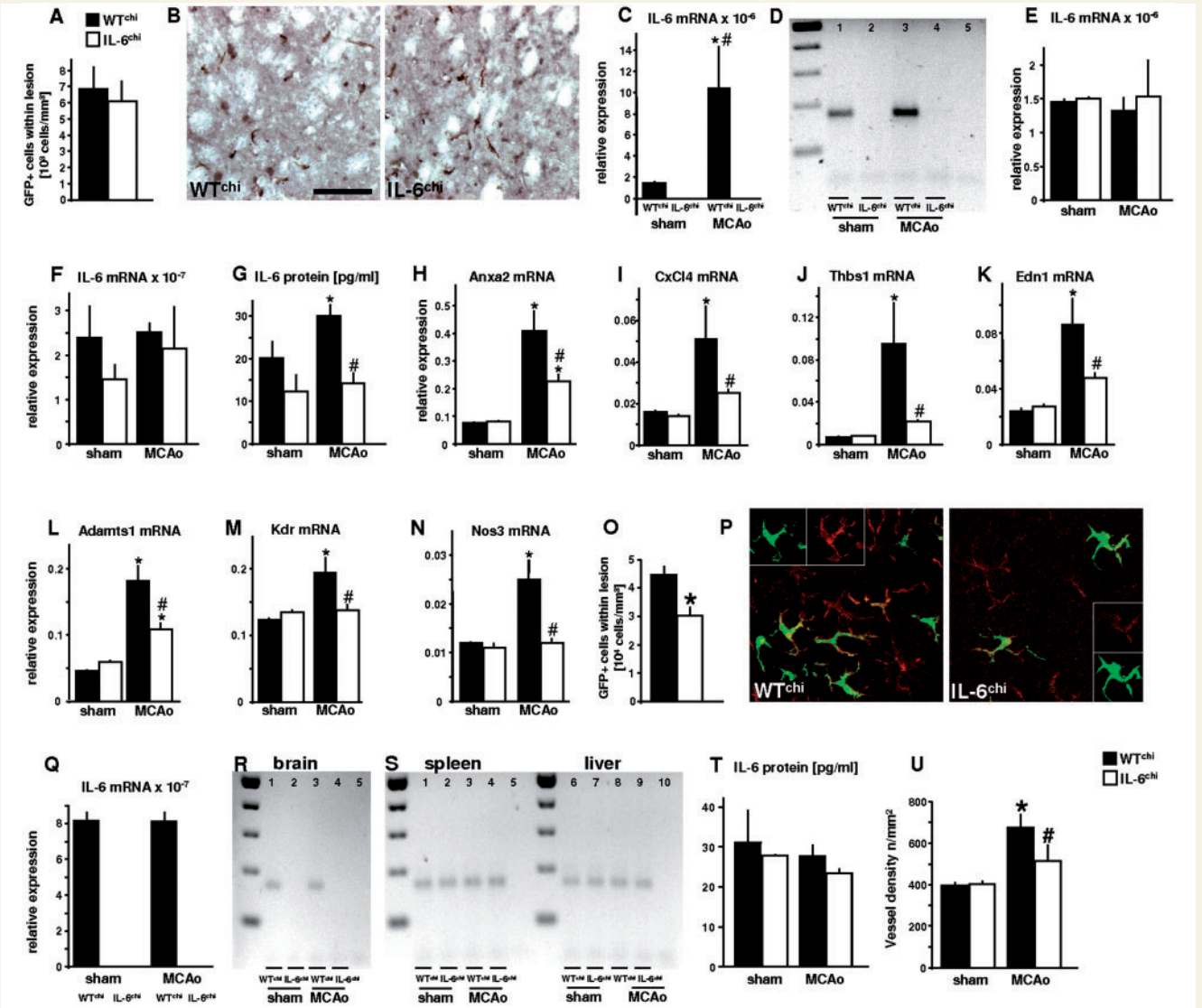

Figure 2 Transplantation of IL-6 competent bone marrow into IL-$6^{-/-}$ mice does not rescue the angiogenic response to transient mild brain ischaemia. (**A–N**) Wild-type mice and IL-$6^{-/-}$ mice were lethally irradiated and then transplanted with bone marrow-derived from ubiquitously 'green' mice [TgN(beta-act-EGFP)1Osb]. All analyses were performed at 48 h after stroke. (**A** and **B**) The number of bone marrow-derived cells in the ischaemic striatum did not differ significantly between chimeric WT^{chi} ($WT^{GFP} \rightarrow$ IL-$6^{+/+}$) and IL-6^{chi} mice ($WT^{GFP} \rightarrow$ IL-$6^{-/-}$). $n = 3$ animals per group. (**C**) Despite engraftment of IL-6 competent bone marrow-derived cells in the ischaemic lesion, we did not detect IL-6 messenger RNA in the brains of IL-6^{chi} mice. In contrast, MCAO elicited a strong increase in IL-6 messenger RNA transcription in the ischaemic lesion in WT^{chi} mice. (**D**) Detection of 174 bp product of IL-6 complementary DNA by gel electrophoresis shows no amplification of an IL-6 specific product in IL-6^{chi} mice. The minus-reverse transcriptase control is shown in lane 5. (**E** and **F**) IL-6 messenger RNA expression in spleen (**E**) and liver (**F**). (**G**) IL-6 protein levels in serum. $n = 2–5$ animals per group. (**H–N**) Expression of key angiogenesis-associated genes in the ischaemic hemisphere. $n = 4–5$ animals per group. (**O–U**) All analyses were performed at 28 days after stroke. (**O** and **P**) The number of bone marrow-derived cells in the ischaemic striatum differed significantly between WT^{chi} and IL-6^{chi} mice. $n = 8–9$ animals per group. (**Q**) Despite engraftment of IL-6 competent bone marrow-derived cells in the ischaemic lesion, we did not detect any IL-6 messenger RNA in the brains of IL-6^{chi} mice. (**R**) Detection of 174 bp product of IL-6 complementary DNA by gel electrophoresis again shows no amplification of an IL-6 specific product in the brain of IL-6^{chi} mice. (**S**) In contrast, IL-6 messenger RNA expression in spleen (*left*) and liver (*right*) is clearly detectable in IL-6^{chi} mice. Minus-reverse transcriptase controls are shown in lane 5 (**R**) as well as in lanes 5 and 10 (**S**). (**T**) IL-6 protein levels in serum. $n = 3–6$ animals per group. (**U**) The density of perfused microvessels was determined using endovascular, auto-fluorescent Evans blue staining and tiled-field imaging. Note significant inducing effect of ischaemia on vessel density in WT^{chi} mice, which was significantly attenuated in IL-6^{chi} mice. $n = 5–6$ animals per group. $^{*}P < 0.05$ relative to sham, $^{\#}P < 0.05$ between recipient genotypes. Scale bar: **B** = 100 μm; **P** = 38 μm.

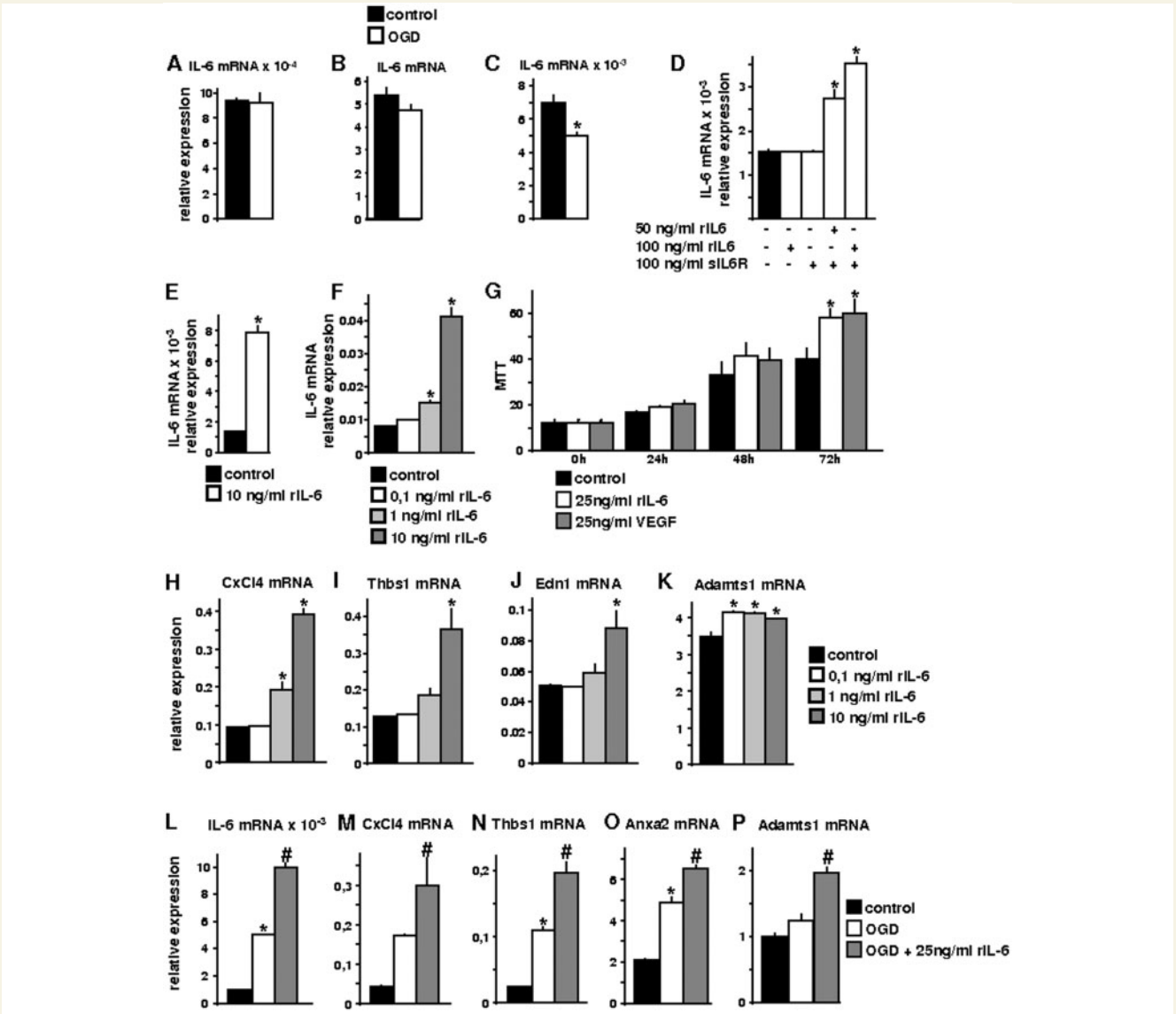

Figure 3 Characterization of the cellular source of IL-6 in brain tissue. Primary cortical neurons, mixed glial cultures and immortalized brain endothelia were subjected to oxygen–glucose deprivation as described in the text (**A–C**). Oxygen–glucose deprivation did not lead to increased IL-6 gene transcription in isolated cultures. Cultures were exposed to recombinant IL-6. Stimulation of primary cortical neurons (**D**), mixed glial cultures (**E**) and of immortalized brain endothelia (**F**) resulted in significantly increased IL-6 messenger RNA transcription. (**G**) Stimulation of bEnd.3 cells by exposure to IL-6 resulted in significantly increased endothelial cell proliferation as measured by MTT conversion and was comparable to VEGF stimulation. Stimulation of bEnd.3 cells by exposure to IL-6 also resulted in significantly increased transcription of key angiogenesis-associated genes *Cxcl4* (**H**), *Thbs1* (**I**), *Edn1* (**J**) and *Adamts1* (**K**). (**L–P**) IL-6 messenger RNA transcription in 350 -μm brain slices was significantly increased at 24 h post oxygen–glucose deprivation and was further increased by cotreatment with recombinant IL-6 (**L**). Correspondingly, transcription of key angiogenesis-associated genes *Cxcl4* (**M**), *Thbs1* (**N**), *Anxa2* (**O**) and *Adamts1* (**P**) was also significantly upregulated in brain slices at 24 h post oxygen–glucose deprivation. Cotreatment with recombinant IL-6 further increased transcription of these genes. All experiments were performed at least in triplicate. $^{*}P < 0.05$ relative to control, $^{\#}P > 0.05$ relative to oxygen–glucose deprivation.

significantly increased at 24 h after MCAO/reperfusion in wild-type mice. Importantly, analysis of subcellular fractions of ischaemic brain tissue from wild-type mice demonstrated a strong increase in phospho-Tyr705-STAT3 both in cytosolic and in nuclear extracts. In contrast, phosphorylation of STAT3 was not increased in ischaemic brain tissue of IL-$6^{-/-}$ mice (Fig. 4). Independent of genotype, we also detected enhanced phosphorylation of AKT especially in cytosolic extracts of ischaemic brain. Finally, we did not detect an effect of either genotype or ischaemia on levels of extracellular signal-regulated kinase 1 and 2 (ERK) or on levels of phosphorylated ERK (pERK) at 24 h after 30 min MCAO. Taken together, these results indicate that wild-type and IL-$6^{-/-}$ mice differ profoundly in the magnitude of STAT3 activation after stroke.

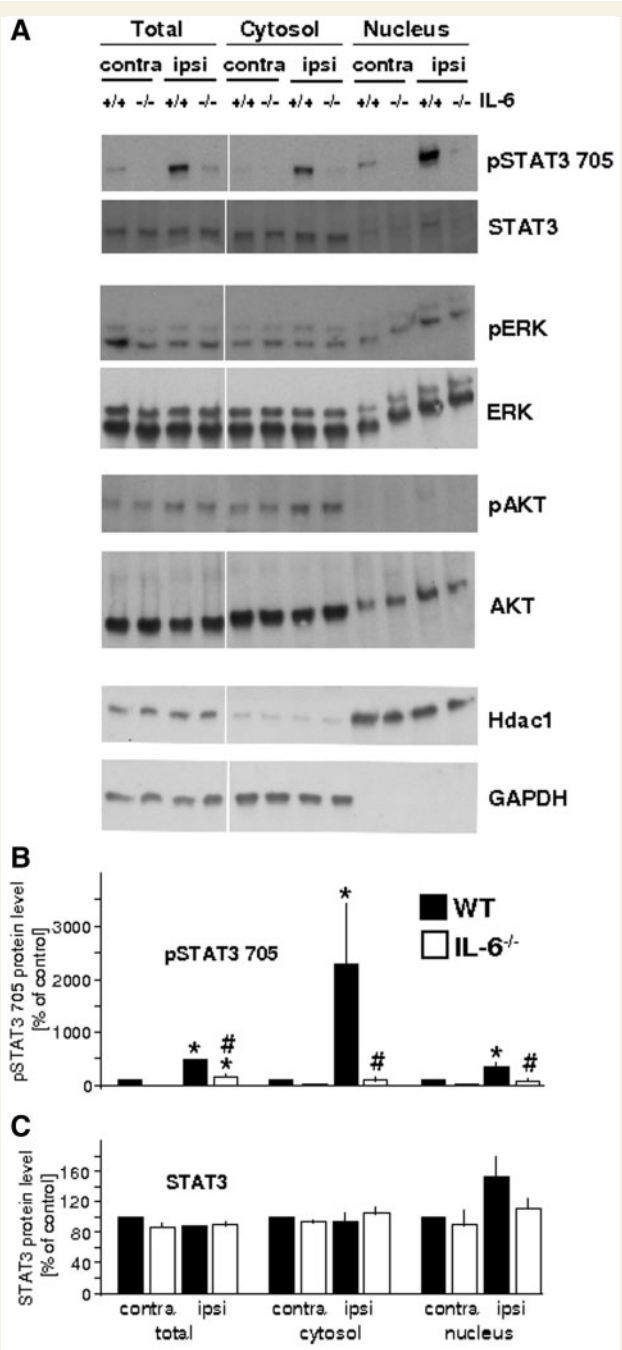

Figure 4 IL-6 deficiency abrogates activation of STAT3 after transient mild brain ischaemia. (**A**) At 24 h after 30 min MCAO/reperfusion, protein expression levels of STAT3, phospho (p)STAT3-705, ERK, pERK, AKT and pAKT were analysed using western blotting. (**B** and **C**) Densitometrical quantification of pSTAT3-705 (**B**) and of total STAT3 (**C**). In wild-type mice, expression of pSTAT3-705 was strongly induced in total protein extracts as well as in both cytosolic and nuclear fractions of ischaemic brain tissue. By contrast, ischaemia-induced STAT3 activation was nearly abolished in IL-$6^{-/-}$ mice. The data are calculated as percentages over contralateral wild-type tissue. $n = 3$ animals per genotype (wild-type versus IL-$6^{-/-}$). Two-way ANOVA [factors: genotype and side of brain (i.e. ipsilateral ischaemic tissue versus contralateral side of brain)] followed by *post hoc* analysis. $^{*}P < 0.05$ for side of brain within genotypes, $^{\#}P < 0.05$ for genotype within side of brain. Hdac1 (nuclear marker protein): histone deacetylase 1. Ipsi = ipsilateral (i.e. ischaemic) brain tissue. Contra = corresponding brain tissue from contralateral hemisphere.

Reduced neovascularization in IL-$6^{-/-}$ mice at 4 weeks after middle cerebral artery occlusion

A 7-day series of daily BrdU injections was begun the day the 30 min MCAO procedure was performed. Histological outcome was evaluated 28 days after MCAO. At this time point, the density of newly generated BrdU-positive cells in ischaemic striatum was significantly reduced in IL-$6^{-/-}$ mice (Fig. 5A and E; Supplementary Fig. 7). Importantly, the percentage of newly generated cells in vessel sites (i.e. von Willebrand factor-associated BrdU-positive cells) was significantly decreased in ischaemic striatum of IL-$6^{-/-}$ mice relative to wild-type controls (Fig. 5E). Also, expression of the endothelial cell marker PECAM-1 was significantly increased in ischaemic brain of wild-type mice relative to IL-$6^{-/-}$ mice (Supplementary Fig. 7F). The further phenotypic characterization of newly generated cells after stroke is summarized in Supplementary Fig. 7.

The density of perfused microvessels was quantified at 28 days after MCAO/reperfusion using endovascular Evans blue staining (Fig. 5B–D and F). Mean arterial blood pressure during Evans blue administration was similar in either genotype (not shown). In wild-type animals, vessel density was increased significantly within the ischaemic striatum compared with the same region on the contralateral side. In contrast, no increase in the density of perfused microvessels within the ischaemic striatum of IL-$6^{-/-}$ mice had occurred at 28 days after transient brain ischaemia (Fig. 5B). Interestingly, IL-6 deficiency also led to alterations of microvascular structure in the ischaemic territory with significantly enlarged vessels (Fig. 5C and F). In additional mice, acetazolamide was administered before sacrifice to induce vasodilation. Independent of genotype, acetazolamide increased average vessel calibre in contralateral striatum. By contrast, in ischaemic striatum, the vascular response was blunted in IL-$6^{-/-}$ mice (Fig. 5D).

As expected, and irrespective of genotype, absolute regional cerebral blood flow was significantly lower in the ischaemic compared with the contralateral striatum at 4 weeks. However, ischaemia-induced reduction in striatal regional cerebral blood flow was significantly more pronounced in IL-$6^{-/-}$ mice relative to wild-type controls (Fig. 5G).

As a further functional parameter, we studied the systemic angiogenic response at 2 weeks after 30 min MCAO/reperfusion using the disc angiogenesis assay. The ingrowth of new vessels into the subcutaneously implanted sponges was significantly reduced in IL-$6^{-/-}$ mice (Fig. 5H and I). Furthermore, the increase in the number of endothelial precursor cells after stroke was significantly blunted in IL-$6^{-/-}$ mice (increase by 15% versus 95% in IL-$6^{+/+}$ animals; $n = 5$–8 animals per group).

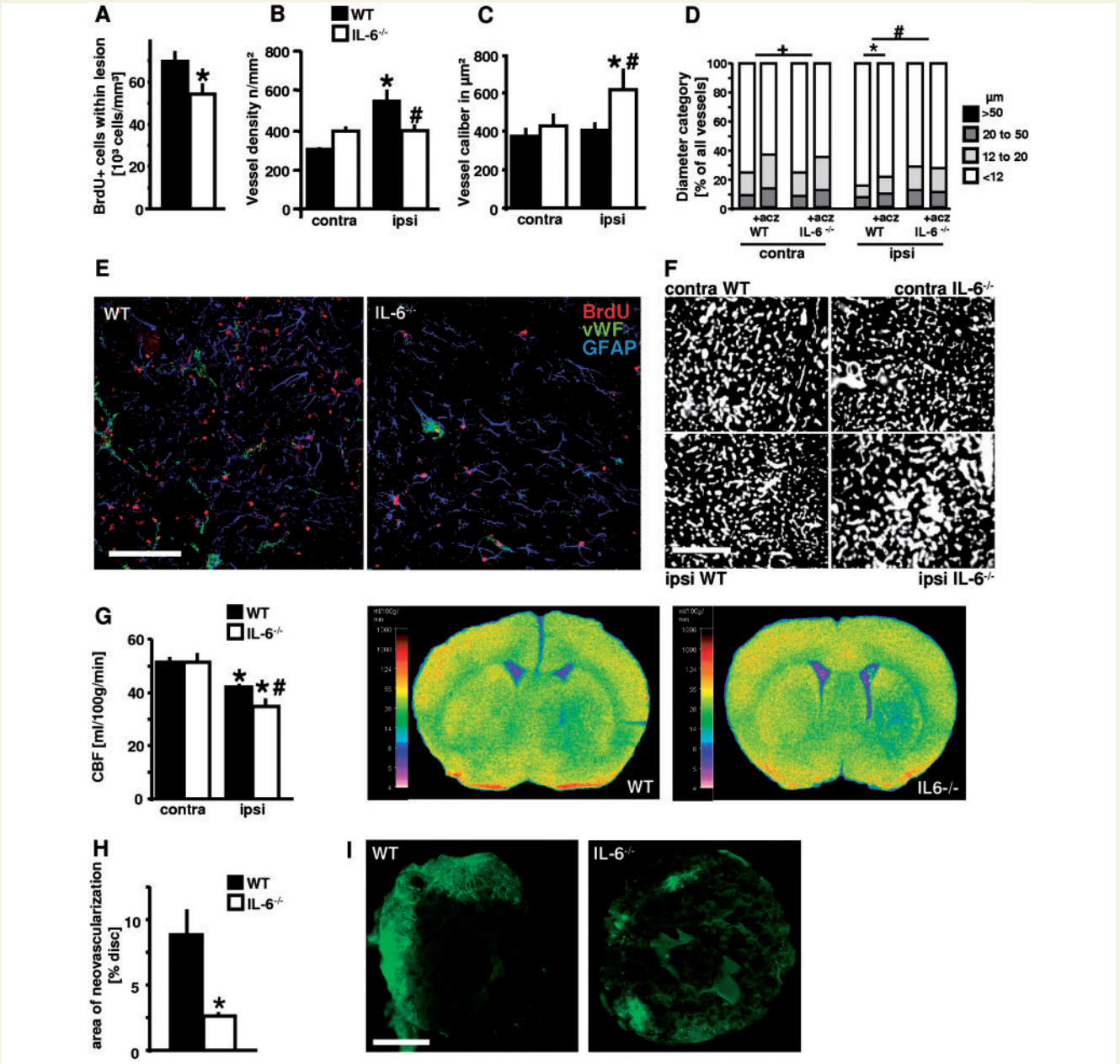

Figure 5 Reduced neovascularization in IL-$6^{-/-}$ mice at 4 weeks after MCAO. (**A** and **E**) Animals received S-phase marker BrdU for seven consecutive days beginning on the day of MCAO. The number of newly generated cells in ischaemic brain was significantly reduced in IL-$6^{-/-}$ mice (**A**). Immunofluorescent staining showed fewer vWF/BrdU-positive cells within the ischaemic lesion of IL-$6^{-/-}$ mice compared with wild-type controls (**E**). *$P < 0.05$ versus wild-type control. Scale bar: **E** = 100 µm. $n = 6$–7 animals per group. (**B**, **C**, **D** and **F**) Effects of IL-6 deficiency on perfused microvessels at 4 weeks following 30 min MCAO. Density (**B**) and average calibre (**C**) of Evans blue-filled vessels were determined using tiled-field mapping and computer-assisted image analysis. (**F**) Representative examples of Evans blue tiled-field images. Note significant inducing effect of ischaemia on vessel density in wild-type mice and on vessel calibre in IL-$6^{-/-}$ mice (**F**). $n = 8$ animals per genotype. *$P < 0.05$ relative to corresponding brain area of contralateral (i.e. non-ischaemic) striatum within each genotype, $^{\#}P < 0.05$ between genotypes within each side. Scale bar: **F** = 500 µm. (**D**) In additional mice, acetazolamide was administered before sacrifice to induce vasodilation. Vessels were categorized according to diameter. Independent of genotype, acetazolamide increased average vessel calibre in contralateral striatum (three-way ANOVA followed by *post hoc* analysis; $^{+}P < 0.05$ for the increase in the 20–50 µm and >50 µm categories and for the decrease in <12 µm category). By contrast, in ischaemic striatum, the vascular response was blunted in IL-$6^{-/-}$ mice (*$P < 0.05$ for the decrease of the <12 µm category; $^{\#}P < 0.05$ for the effect of genotype in ischaemic striatum on the <12, 12–20, 20–50 and >50 -µm categories). $n = 3$–5 mice per group. (**G**) Cerebral blood flow was measured in ischaemic striatum (ipsi) and corresponding area of contralateral hemisphere (contra) at 4 weeks after 30 min MCAO using ^{14}C-iodoantipyrine tissue equilibration technique. Analysis of $n = 10$ mice per group. *$P < 0.05$ relative to contralateral striatum, $^{\#}P < 0.05$ between genotypes within the ischaemic striatum. (**H** and **I**) The systemic angiogenic response after brain ischaemia was assessed in a bioassay of disc angiogenesis. The area of neovascularization was significantly reduced in IL-$6^{-/-}$ mice. $n = 4$ mice per group. *$P < 0.05$ versus wild-type control. Scale bar: **I** = 2 mm.

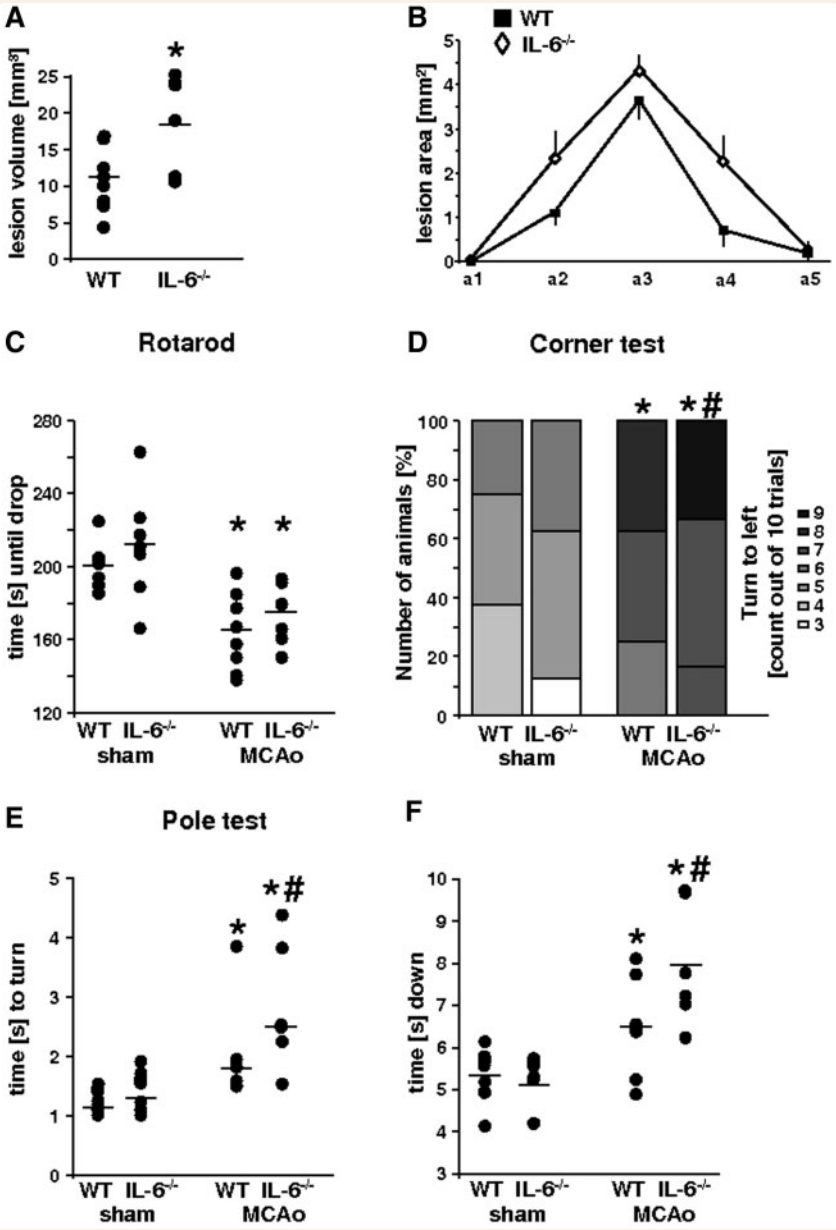

Figure 6 Increased chronic lesion volumes and worse functional outcome in IL-$6^{-/-}$ mice after mild cerebral ischaemia. Neuronal damage was assessed at 4 weeks after MCAO/reperfusion using NeuN immunohistochemistry. Cerebral lesion volumes are presented as individual data points (**A**). Direct cerebral lesion areas (**B**) were determined on five coronal brain sections (approximately interaural 6.6, 5.3, 3.9, 1.9 and -0.1 mm, respectively) by computer-assisted volumetry. Note that IL-$6^{-/-}$ mice show significantly enlarged chronic lesion volumes. *$P < 0.05$ versus wild-type. (**C**) Independent of genotype, MCAO animals showed worse Rotarod performance at 72 h post-stroke. (**D**) Behavioural asymmetries were assessed at 22 days after MCAO on the corner test. (**E**) Time to turn and (**F**) time to reach the floor at 23 days after MCAO on the pole test. Values are presented as individual data points (**C**, **E** and **F**) or as the percentage of animals that had performed the respective number of left turns (**D**). Horizontal bars = means. *$P < 0.05$ relative to sham, $^{\#}P < 0.05$ within genotypes. WT = wild-type.

IL-6 deficiency confers increased chronic lesion size and impaired functional outcome after mild stroke

Acute stroke outcome was assessed at 48 h after 30 min MCAO/reperfusion. In line with two earlier reports (Clark *et al.*, 2000; Herrmann *et al.*, 2003), acute lesion volumes (mm^3) did not differ significantly between genotypes (wild-type: 49.7 ± 7.9; IL-$6^{-/-}$: 51.1 ± 9.6; $n = 5$–7 per genotype). Similarly, Rotarod performance assessed at 72 h after MCAO also did not differ between genotypes (Fig. 6C). In contrast, at 28 days after MCAO, NeuN immunostaining demonstrated significantly increased lesion sizes in IL-$6^{-/-}$ mice (Fig. 6A and B). Increased chronic lesion

volumes and the deficit in post-stroke angiogenesis in IL-6$^{-/-}$ mice were associated with increased behavioural asymmetries on the corner test (Fig. 6D), as well as with significantly increased times to turn and to reach the floor on the pole test (Fig. 6E and F).

Discussion

This study demonstrates the essential role of IL-6 produced locally by resident brain cells for post-stroke angiogenesis. First, at 2 days after mild transient brain ischaemia, wild-type mice showed a significant early increase in IL-6 gene transcription and in IL-6 protein levels in ischaemic brain that was accompanied by a significant early upregulation of angiogenesis-associated genes. In IL-6$^{-/-}$ mice, these early genomic changes in angiogenesis-related gene networks were strongly blunted.

Secondly, experiments in culture and in bone marrow-chimeric mice yielded complementary evidence that resident brain cells serve as the major source of IL-6 after stroke. Importantly, neither at 48 h nor at 4 weeks after brain ischaemia did we detect any IL-6 gene transcription in the brains of IL-6$^{-/-}$ mice reconstituted with IL-6 competent bone marrow. Furthermore, cell culture experiments uncovered a self-enhancing process of IL-6 production in isolated neurons and glia as well as in organotypic brain slices.

Thirdly, while ischaemia caused phosphorylation of STAT3 at Tyr705 in wild-type mice, IL-6 deficiency inhibited early STAT3 activation in ischaemic brain tissue.

Fourth, wild-type mice showed a strong proliferative reaction in the ischaemic brain with increased numbers of newborn cells in vessel sites. This proliferative response was significantly reduced in IL-6$^{-/-}$ mice. Additionally, the systemic angiogenic response as measured by disc neovascularization as well as by the increase in endothelial progenitor cells after MCAO was significantly blunted in IL-6$^{-/-}$ mice. Consequently, density of perfused microvessels at 4 weeks after stroke was significantly increased in the brains of wild-type, but not of IL-6$^{-/-}$ mice. Furthermore, acetazolamide failed to increase vessel calibres in ischaemic striatum of IL-6$^{-/-}$ mice, indicative of chronically compromised vascular responsivity.

Finally although acute stroke outcome did not differ between genotypes, IL-6$^{-/-}$ mice displayed significantly larger lesion volumes and a worse sensorimotor outcome after 4 weeks.

The origin of the surge in circulating IL-6 levels in stroke has been debated for some time (Dziedzic *et al.*, 2003). A number of previous studies hinted at neurons, glial cells and the vascular endothelium to be the source of IL-6 after brain ischaemia (Suzuki *et al.*, 2009). Here, we clearly show that IL-6 competent bone marrow-derived cells are not sufficient to rescue IL-6 expression in ischaemic brain of IL-6$^{-/-}$ mice. Also, IL-6 competent IL-6^{chi} mice did not display increased IL-6 protein levels in serum at 48 h after stroke. Consequently, activation of key angiogenesis-associated genes in ischaemic brain was not rescued in IL-6^{chi} mice. Accordingly, chronic stroke outcome in IL-6^{chi} mice recapitulated the major effects of IL-6 deficiency on post-stroke regeneration with significantly enhanced lesion volumes and reduced vessel densities. Additional *in vitro* experiments yielded complementary evidence that after stroke, resident brain cells serve as the major source of IL-6 in a self-amplifying network. Importantly, oxygen–glucose deprivation of organotypic brain slices resulted not only in increased IL-6 messenger RNA transcription, but also in the upregulation of key angiogenesis-associated genes identified by genomic profiling of ischaemic brain tissue. Administration of recombinant IL-6 to brain slices after oxygen–glucose deprivation further significantly increased transcription of all these genes demonstrating a gain of function mechanism.

Admittedly, our results do not allow us to pinpoint exactly the primary cellular source of IL-6 production in the ischaemic brain. However, it is likely that 'damage'-associated molecular patterns—possibly in concert with neurotransmitters and endogenous nucleotides released first from dying neurons, the most vulnerable cell type in brain—lead to an initial release of IL-6 and other cytokines from resident glia. Notably, microglial activation by oxygen–glucose deprivation-stressed neurons and by necrotic neurons has previously been reported (Kaushal and Schlichter, 2008; Pais *et al.*, 2008). Our data show that this initial IL-6 release can then be amplified by all major cell types in the brain.

We acknowledge that our study does not include a genuine 'rescue experiment' in the sense that we have not shown that IL-6 rescues impaired angiogenesis in IL-6$^{-/-}$ mice after stroke. However, such a rescue experiment is by no means as straightforward as it might seem. Importantly, as detailed above, IL-6 drives a self-amplification loop that is likely to be hard to replicate *in vivo* in IL-6-deficient brains. In particular, dynamic temporospatial changes in IL-6 levels after stroke would have to be modelled. Therefore, a simplistic 'add-back' experiment with either intraperitoneal or intracerebroventricular administration of IL-6 does not seem to be adequate. In the first instance, the hugely divergent roles of central and peripheral IL-6 in the inflammatory response to brain ischaemia would seriously confound the interpretation of results (Karelina *et al*., 2009). In the second instance, different degrees of local inflammation and tissue damage secondary to implantation of mini-osmotic pumps will inevitably lead to high variability in the expression of angiogenesis-associated genes. Furthermore, the use of mini-osmotic pumps also raises the problem of the stability of recombinant IL-6 for prolonged periods of time.

A number of studies have reported a strong nexus between neovascularization and activation and recruitment of microglia/macrophages (Jander *et al*., 1998; Manoonkitiwongsa *et al*., 2001; Welser *et al*., 2010). Another interesting finding from our experiments in chimeric mice is therefore that the invasion of bone marrow-derived cells into the ischaemic brain is significantly reduced in IL-6^{chi} mice at 4 weeks after MCAO. This observation fits well with an *in vitro* study demonstrating that IL-6 promotes migration of monocytes through an endothelial cell layer (Clahsen and Schaper, 2008). In this context, it is also interesting to note that IL-6 deficiency resulted in reduced gene transcription of *Jam-1*, *ICAM1*, *PECAM-1* and *VE-Cadherin* at 48 h after stroke. All these genes have been implicated in a molecular network governing endothelium-dependent leucocyte transmigration (Muller *et al.*, 2011).

In the context of deficient regenerative angiogenesis, our finding of reduced STAT3 phosphorylation in IL-6$^{-/-}$ mice fits well with earlier reports demonstrating that phosphorylation of STAT3 is essential for endothelial cell migration as well as tube and vessel

formation (Yahata *et al.*, 2003; Wani *et al.*, 2011). Importantly, IL-6 has recently been shown to induce STAT3 phosphorylation in endothelial progenitor cells and to promote endothelial progenitor cell proliferation, migration and Matrigel^{TM} tube formation (Fan *et al.*, 2008). Furthermore, IL-6 has been demonstrated to induce the expression of VEGF, consistent with our finding that the increase in circulating VEGF levels at 48 h after MCAO is reduced in IL-6$^{-/-}$ mice (Cohen *et al.*, 1996). STAT3 has also been shown to serve as an important regulator of astrogliosis and scar formation (Herrmann *et al.*, 2008). Interestingly, despite the reduction of STAT3 activation, we did not detect a reduction in glial fibrillary acidic protein messenger RNA or protein expression in IL-6$^{-/-}$ mice. It is likely that under the conditions of brain ischaemia, other signalling pathways such as Akt may largely compensate for reduced STAT3 activation in astrocytes (Namura *et al.*, 2000; Franke *et al.*, 2009).

Finally, our combined data indicate that ischaemia elicits an early transient activation of angiogenesis-related gene networks. Obviously, angiogenesis is a complex multi-step process, extending over many weeks after stroke. However, the strongest activation of angiogenesis-related genes occurs early after brain ischaemia. Furthermore, the effects of IL-6 deficiency on angiogenesis-related gene transcription also emerged most clearly early after stroke. Whereas angiogenesis genes as a class did not differ between genotypes in sham-operated animals, the mild ischaemic stimulus unmasked pronounced genomic effects of IL-6 deficiency with a largely suppressed angiogenic response in IL-6 deficient brain. Conversely, exposure of immortalized brain endothelia to IL-6 upregulated several key angiogenesis-associated genes identified initially by genomic profiling. Since microarray analyses were performed from coronal hemisections of whole brain, our data do not permit us to gauge precisely the relative contribution of specific cell types to the activation of angiogenesis-related gene networks. Interestingly, however, the genotype effect disappeared with severe ischaemia. Unlike in the mild ischaemia model, where tissue damage is relatively selective for neurons and confined to the lateral striatum, the lesion produced by 60 min MCAO is severe (pannecrosis) and involves both neurons and glia (including endothelia) in the entire middle cerebral artery territory. One explanation for the discrepancy of our results between the 30 and 60 min MCAO models is that IL-6 promotes angiogenesis and regeneration by enlisting surviving glia, especially in peri-infarct tissue. Our results indicate that circulating IL-6 levels in human stroke patients, which have been suggested as a predictive biomarker, should also be judged in the context of stroke severity and stroke duration.

In line with reduced activation of angiogenesis-related genes early after stroke, IL-6$^{-/-}$ mice displayed fewer numbers of newly generated cells in vessel sites. Accordingly, the density of perfused (i.e. functionally intact) vessels was also decreased in ischaemic striatum of IL-6$^{-/-}$ mice relative to wild-type controls. Interestingly, microvessels in ischaemic brain of IL-6$^{-/-}$ mice also showed morphological alterations and a reduced vasodilatory response to acetazolamide. Taken together, these results indicate that IL-6 deficiency profoundly impairs angiogenesis after stroke. Formation of new vessels in the ischaemic brain is a critical mechanism that fosters long-term recovery and regeneration. We have previously demonstrated that regular physical activity augments neovascularization as well as cerebral blood flow after stroke (Gertz *et al.*, 2006). Importantly, in that earlier study, smaller lesion sizes and improved functional outcome associated with physical activity were completely abrogated when angiogenesis was blocked. Similarly, the perturbed angiogenic response in IL-6$^{-/-}$ mice observed here was associated with increased chronic lesion areas and worse functional recovery.

In conclusion, IL-6 promotes early transcriptomic changes in angiogenesis-related gene networks after brain ischaemia, which leads to increased angiogenesis during the delayed phases after experimental stroke. IL-6 thereby affords long-term histological and functional protection. Our study highlights the importance of neuroinflammation for chronic post-stroke recovery.

Acknowledgements

We thank Bettina Herrmann, Nadja Strahl, Melanie Kroh, Annemarie Bunge, Anke Sänger, Raymond Monk, Anneke Telkamp, Ellen Becker and Marco Foddis for excellent technical assistance. Christoph Harms provided valuable advice on primer design. We thank Markus Schwaninger for initially supplying IL-6 knockout mice.

Funding

The Deutsche Forschungsgemeinschaft (SFB TRR43 and Cluster of Excellence NeuroCure EXC 257 to M.E., U.D. and F.L.H.), the VolkswagenStiftung (Lichtenberg Programme to M.E.), the Bundesministerium für Bildung und Forschung (Centre for Stroke Research Berlin), the European Union's Seventh Framework Programme (FP7/2008-2013) under grant agreements n° 201024 and n° 202213 (European Stroke Network) and by the US National Institutes of Health (NINDS R01 NS046006 to F.L.H.).

Supplementary material

Supplementary material is available at *Brain* online.

References

Acalovschi D, Wiest T, Hartmann M, Farahmi M, Mansmann U, Auffarth GU, et al. Multiple levels of regulation of the interleukin-6 system in stroke. Stroke 2003; 34: 1864–9.

Andjelkovic AV, Stamatovic SM, Keep RF. The protective effects of preconditioning on cerebral endothelial cells in vitro. J Cereb Blood Flow Metab 2003; 23: 1348–55.

Azari BM, Marmur JD, Salifu MO, Ehrlich YH, Kornecki E, Babinska A. Transcription and translation of human F11R gene are required for an initial step of atherogenesis induced by inflammatory cytokines. J Transl Med 2011; 9: 98.

Bromberg J, Darnell JE Jr. The role of STATs in transcriptional control and their impact on cellular function. Oncogene 2000; 19: 2468–73.

Carmeliet P, Lampugnani MG, Moons L, Breviario F, Compernolle V, Bono F, et al. Targeted deficiency or cytosolic truncation of the

VE-cadherin gene in mice impairs VEGF-mediated endothelial survival and angiogenesis. Cell 1999; 98: 147–57.

Chen J, Cui X, Zacharek A, Roberts C, Chopp M. eNOS mediates TO90317 treatment-induced angiogenesis and functional outcome after stroke in mice. Stroke 2009; 40: 2532–8.

Chourbaji S, Urani A, Inta I, Sanchis-Segura C, Brandwein C, Zink M, et al. IL-6 knockout mice exhibit resistance to stress-induced development of depression-like behaviors. Neurobiol Dis 2006; 23: 587–94.

Clahsen T, Schaper F. Interleukin-6 acts in the fashion of a classical chemokine on monocytic cells by inducing integrin activation, cell adhesion, actin polymerization, chemotaxis, and transmigration. J Leukoc Biol 2008; 84: 1521–9.

Clark WM, Rinker LG, Lessov NS, Hazel K, Hill JK, Stenzel-Poore M, et al. Lack of interleukin-6 expression is not protective against focal central nervous system ischemia. Stroke 2000; 31: 1715–20.

Cohen T, Nahari D, Cerem LW, Neufeld G, Levi BZ. Interleukin 6 induces the expression of vascular endothelial growth factor. J Biol Chem 1996; 271: 736–41.

DeLisser HM, Christofidou-Solomidou M, Strieter RM, Burdick MD, Robinson CS, Wexler RS, et al. Involvement of endothelial PECAM-1/CD31 in angiogenesis. Am J Pathol 1997; 151: 671–7.

Dziedzic T, Slowik A, Szczudlik A. Interleukin-6 and stroke: cerebral ischemia versus nonspecific factors influencing interleukin-6. Stroke 2003; 34: e229.

Endres M, Biniszkiewicz D, Sobol RW, Harms C, Ahmadi M, Lipski A, et al. Increased postischemic brain injury in mice deficient in uracil-DNA glycosylase. J Clin Invest 2004; 113: 1711–21.

Endres M, Fan G, Hirt L, Fujii M, Matsushita K, Liu X, et al. Ischemic brain damage in mice after selectively modifying BDNF or NT4 gene expression. J Cereb Blood Flow Metab 2000a; 20: 139–44.

Endres M, Gertz K, Lindauer U, Katchanov J, Schultze J, Schröck H, et al. Mechanisms of stroke protection by physical activity. Ann Neurol 2003; 545: 582–90.

Endres M, Meisel A, Biniszkiewicz D, Namura S, Prass K, Ruscher K, et al. DNA methyltransferase contributes to delayed ischemic brain injury. J Neurosci 2000b; 20: 3175–81.

Fan Y, Ye J, Shen F, Zhu Y, Yeghiazarians Y, Zhu W, et al. Interleukin-6 stimulates circulating blood-derived endothelial progenitor cell angiogenesis in vitro. J Cereb Blood Flow Metab 2008; 28: 90–8.

Franke H, Sauer C, Rudolph C, Krügel U, Hengstler JG, Illes P. P2 receptor-mediated stimulation of the PI3-K/Akt-pathway in vivo. Glia 2009; 57: 1031–45.

Gallucci RM, Simeonova PP, Matheson JM, Kommineni C, Guriel JL, Sugawara T, et al. Impaired cutaneous wound healing in interleukin-6-deficient and immunosuppressed mice. FASEB J 2000; 14: 2525–31.

Gertz K, Priller J, Kronenberg G, Winter B, Schröck H, Ji S, et al. Physical activity improves long-term stroke outcome via eNOS-dependent augmentation of neo-vascularization and cerebral blood flow. Circ Res 2006; 99: 1132–40.

Göbel U, Theilen H, Kuschinsky W. Congruence of total and perfused capillary network in rat brains. Circ Res 1990; 66: 271–81.

Grathwohl SA, Kälin RE, Bolmont T, Prokop S, Winkelmann G, Kaeser SA, et al. Formation and maintenance of Alzheimer's disease beta-amyloid plaques in the absence of microglia. Nat Neurosci 2009; 12: 1361–3.

Harhausen D, Prinz V, Ziegler G, Gertz K, Endres M, Lehrach H, et al. CD93/AA4.1: a novel regulator of inflammation in murine focal cerebral ischemia. J Immunol 2010; 184: 6407–17.

Harms C, Albrecht K, Harms U, Seidel K, Hauck L, Baldinger T, et al. Phosphatidylinositol 3-Akt-kinase-dependent phosphorylation of p21(Waf1/Cip1) as a novel mechanism of neuroprotection by glucocorticoids. J Neurosci 2007; 27: 4562–71.

Harms C, Lautenschlager M, Bergk A, Freyer D, Weih M, Dirnagl U, et al. Melatonin is protective in necrotic but not in caspase-dependent, free radical-independent apoptotic neuronal cell death in primary neuronal cultures. FASEB J 2000; 14: 1814–24.

Heinrich P, Behrmann I, Haan S, Hermanns H, Müller-Newen G, Schaper F. Principles of interleukin (IL)-6-type cytokine signalling and its regulation. Biochem J 2003; 374: 1–20.

Heinrich PC, Behrmann I, Müller-Newen G, Schaper F, Graeve L. Interleukin-6-type cytokine signaling through the gp130/Jak/STAT pathway1. Biochem J 2002; 334: 297–314.

Heppner FL, Greter M, Marino D, Falsig J, Raivich G, Hövelmeyer N, et al. Experimental autoimmune encephalomyelitis repressed by microglial paralysis. Nat Med 2005; 11: 146–52.

Herrmann JE, Imura T, Song B, Qi J, Ao Y, Nguyen TK, et al. STAT3 is a critical regulator of astrogliosis and scar formation after spinal cord injury. J Neurosci 2008; 28: 7231–43.

Herrmann O, Tarabin V, Suzuki S, Attigah N, Coserea I, Schneider A, et al. Regulation of body temperature and neuroprotection by endogenous interleukin-6 in cerebral ischemia. J Cereb Blood Flow Metab 2003; 23: 406–15.

Hirano T, Ishihara K, Hibi M. Roles of STAT3 in mediating the cell growth, differentiation and survival signals relayed through the IL-6 family of cytokine receptors. Oncogene 2000; 19: 2548–56.

Jander S, Schroeter M, D'Urso D, Gillen C, Witte OW, Stoll G. Focal ischaemia of the rat brain elicits an unusual inflammatory response: early appearance of CD8+ macrophages/microglia. Eur J Neurosci 1998; 10: 680–8.

Ji S, Kronenberg G, Balkaya M, Färber K, Gertz K, Kettenmann H, et al. Acute neuroprotection by pioglitazone after mild brain ischemia without effect on long-term outcome. Exp Neurol 2009; 216: 321–8.

Jüttler E, Tarabin V, Schwaninger M. Interleukin-6 (Il-6): a possible neuromodulation induced by neuronal activity. The Neuroscientist 2002; 8: 268–75.

Karelina K, Norman GJ, Zhang N, Morris JS, Peng H, DeVries AC. Social isolation alters neuroinflammatory response to stroke. Proc Natl Acad Sci USA 2009; 106: 5895–900.

Katchanov J, Waeber C, Gertz K, Gietz A, Winter B, Brück W, et al. Selective neuronal vulnerability following mild focal brain ischemia in the mouse. Brain Pathol 2003; 13: 452–64.

Kaushal V, Schlichter LC. Mechanisms of microglia-mediated neurotoxicity in a new model of the stroke penumbra. J Neurosci 2008; 28: 2221–30.

Kevil CG, Orr AW, Langston W, Mickett K, Murphy-Ullrich J, Patel RP, et al. Intercellular adhesion molecule-1 (ICAM-1) regulates endothelial cell motility through a nitric oxide-dependent pathway. J Biol Chem 2004; 279: 19230–8.

Kopf M, Baumann H, Freer G, Freudenberg M, Lamers M, Kishimoto T, et al. Impaired immune and acute-phase responses in interleukin-6-deficient mice. Nature 1994; 368: 339–42.

Kronenberg G, Reuter K, Steiner B, Brandt MD, Jessberger S, Yamaguchi M, et al. Subpopulations of proliferating cells of the adult hippocampus respond differently to physiologic neurogenic stimuli. J Comp Neurol 2003; 467: 455–63.

Kronenberg G, Wang LP, Synowitz M, Gertz K, Katchanov J, Glass R, et al. Nestin-expressing cells divide and adopt a complex electrophysiologic phenotype after transient brain ischemia. J Cereb Blood Flow Metab 2005; 25: 1613–24.

Laufs U, Werner N, Link A, Endres M, Wassmann S, Jürgens C, et al. Physical training increases endothelial progenitor cells, inhibits neointima formation, and enhances angiogenesis. Circulation 2004; 109: 220–6.

Lautenschlager M, Onufriev MV, Gulyaeva NV, Harms C, Freyer D, Sehmsdorf U, et al. Role of nitric oxide in the ethylcholine aziridinium model of delayed apoptotic neurodegeneration in vivo and in vitro. Neuroscience 2000; 97: 383–93.

Levy DE, Lee CK. What does Stat3 do? J Clin Invest 2002; 109: 1143–8.

Lin ZQ, Kondo T, Ishida Y, Takayasu T, Mukaida N. Essential involvement of IL-6 in the skin wound-healing process as evidenced by delayed wound healing in IL-6-deficient mice. J Leukoc Biol 2003; 73: 713–21.

Loddick SA, Turnbull AV, Rothwell NJ. Cerebral interleukin-6 is neuroprotective during permanent focal cerebral ischemia in the rat. J Cereb Blood Flow Metab 1998; 18: 176–9.

Maeda K, Hata R, Hossmann KA. Differences in the cerebrovascular anatomy of C57black/6 and SV129 mice. Neuroreport 1998; 9: 1317–9.

Manoonkitiwongsa PS, Jackson-Friedman C, McMillan PJ, Schultz RL, Lyden PD. Angiogenesis after stroke is correlated with increased numbers of macrophages: the clean-up hypothesis. J Cereb Blood Flow Metab 2001; 21: 1223–31.

Muller WA. Mechanisms of leukocyte transendothelial migration. Annu Rev Pathol 2011; 6: 323–44.

Nagai N, Yamamoto S, Tsuboi T, Ihara H, Urano T, Takada Y, et al. Tissue-type plasminogen activator is involved in the process of neuronal death induced by oxygen-glucose deprivation in culture. J Cereb Blood Flow Metab 2001; 21: 631–4.

Naik MU, Mousa SA, Parkos CA, Naik UP. Signaling through JAM-1 and alphavbeta3 is required for the angiogenic action of bFGF: dissociation of the JAM-1 and alphavbeta3 complex. Blood 2003; 102: 2108–14.

Namura S, Nagata I, Kikuchi H, Andreucci M, Alessandrini A. Serine-threonine protein kinase Akt does not mediate ischemic tolerance after global ischemia in the gerbil. J Cereb Blood Flow Metab 2000; 20: 1301–5.

Navaratna D, Guo S, Arai K, Lo EH. Mechanisms and targets for angiogenic therapy after stroke. Cell Adh Migr 2009; 3: 216–23.

Nian M, Lee P, Khaper N, Liu P. Inflammatory cytokines and postmyocardial infarction remodelling. Circ Res 2004; 94: 1543–53.

Nishida Y, Sugahara-Kobayashi M, Takahashi Y, Nagata T, Ishikawa K, Asai S. Screening for control genes in mouse hippocampus after transient forebrain ischemia using high-density oligonucleotide array. J Pharmacol Sci 2006; 101: 52–7.

Pais TF, Figueiredo C, Peixoto R, Braz MH, Chatterjee S. Necrotic neurons enhance microglial neurotoxicity through induction of glutaminase by a MyD88-dependent pathway. J Neuroinflammation 2008; 5: 43.

Planas AM, Gorina R, Chamorro A. Signalling pathways mediating inflammatory responses in brain ischaemia. Biochem Soc Trans 2006; 34: 1267–70.

Pohlers M, Truss M, Frede U, Scholz A, Strehle M, Kuban RJ, et al. A role for E2F6 in the restriction of male-germ-cell-specific gene expression. Curr Biol 2005; 15: 1051–7.

Reyes TM, Fabry Z, Coe CL. Brain endothelial cell production of a neuroprotective cytokine, interleukin-6, in response to noxious stimuli. Brain Res 1999; 851: 215–20.

Schobitz B, de Kloet ER, Sutanto W, Holsboer F. Cellular localization of interleukin 6 mRNA and interleukin 6 receptor mRNA in rat brain. Eur J Neurosci 1993; 5: 1426–35.

Smith CJ, Emsley HC, Gavin CM, Vail A, Barberan EM, del Zoppo GJ, et al. Peak plasma interleukin-6 and other peripheral markers of inflammation in the first week of ischaemic stroke correlate with brain infarct volume, stroke severity and long-term outcome. BMC Neurol 2004; 4: 2.

Suzuki S, Tanaka K, Suzuki N. Ambivalent aspects of interleukin-6 in cerebral ischemia: inflammatory versus neurotrophic aspects. J Cereb Blood Flow Metab 2009; 29: 464–79.

Van Wagoner NJ, Oh JW, Repovic P, Benveniste EN. Interleukin-6 (IL-6) production by astrocytes: autocrine regulation by IL-6 and the soluble IL-6 receptor. J Neurosci 1999; 19: 5236–44.

Waje-Andreassen U, Kråkenes J, Ulvestad E, Thomassen L, Myhr KM, Aarseth J, et al. IL-6: an early marker for outcome in acute ischemic stroke. Acta Neurol Scand 2005; 111: 360–5.

Wani AA, Jafarnejad SM, Zhou J, Li G. Integrin-linked kinase regulates melanoma angiogenesis by activating NF-κB/interleukin-6 signaling pathway. Oncogene 2011; 30: 2778–88.

Welser JV, Li L, Milner R. Microglial activation state exerts a biphasic influence on brain endothelial cell proliferation by regulating the balance of TNF and TGF-β1. J Neuroinflammation 2010; 7: 89.

Werner C, Kamani CH, Gensch C, Böhm M, Laufs U. The peroxisome proliferator-activated receptor-gamma agonist pioglitazone increases number and function of endothelial progenitor cells in patients with coronary artery disease and normal glucose tolerance. Diabetes 2007; 56: 2609–15.

Woodroofe MN, Sarna GS, Wadha M, Hayes GM, Loughlin AJ, Tinker A, et al. Detection of interleukin-1 and interleukin-6 in adult rat brain, following mechanical injury, by in vivo microdialysis: evidence of a role for microglia in cytokine production. J Neuroimmunol 1991; 33: 227–36.

Yahata Y, Shirakata Y, Tokumaru S, Yamasaki K, Sayama K, Hanakawa Y, et al. Nuclear translocation of phosphorylated STAT3 is essential for vascular endothelial growth factor-induced human dermal microvascular endothelial cell migration and tube formation. J Biol Chem 2003; 278: 40026–31.

Yamashita T, Sawamoto K, Suzuki S, Suzuki N, Adachi K, Kawase T, et al. Blockade of interleukin-6 signalling aggravates ischemic cerebral damage in mice: possible involvement of Stat3 activation in the protection of neurons. J Neurochem 2005; 94: 459–68.

Zhang L, Schallert T, Zhang ZG, Jiang Q, Arniego P, Li Q, et al. A test for detecting long-term sensorimotor dysfunction in the mouse after focal cerebral ischemia. J Neurosci Methods 2002; 117: 207–14.

Zhao BQ, Wang S, Kim H-Y, Storrie H, Rosen BR, Mooney DJ, et al. Role of matrix metalloproteinases in delayed cortical responses after stroke. Nat Med 2006; 12: 441–5.